

NPS ARCHIVE
1966
TRIEBES, C.

AN INVESTIGATION OF THE S/N FATIGUE GAGE

by

CARL J. TRIEBES, JR.

B.S. United States Naval Academy
(1958)

SUBMITTED IN PARTIAL FULFILLMENT OF THE

REQUIREMENTS FOR THE DEGREES OF

MASTER OF SCIENCE

IN NAVAL ARCHITECTURE AND MARINE ENGINEERING

AND

NAVAL ENGINEER

at the

MASSACHUSETTS INSTITUTE OF TECHNOLOGY

June 1966

Thesis
T797

DUDLEY KNOX LIBRARY
NAVAL POSTGRADUATE SCHOOL
MONTEREY, CA 93943-5101

AN INVESTIGATION OF THE S/N FATIGUE CASE

by

CARL JOHN TRIBBES, JR.

B.S. United States Naval Academy
(1958)

SUBMITTED IN PARTIAL FULFILLMENT OF THE
REQUIREMENTS FOR THE DEGREE OF
MASTER OF SCIENCE
IN NAVAL ARCHITECTURE AND MARINE ENGINEERING
AND
NAVAL ENGINEER

at the

MASSACHUSETTS INSTITUTE OF TECHNOLOGY

June 1966

AN INVESTIGATION OF THE S/N FATIGUE GAGE

by

Carl John Triebs, Jr.

Submitted to the Department of Naval Architecture and Marine Engineering on May 20, 1966, in partial fulfillment of the requirements for the Master of Science Degree in Naval Architecture and Marine Engineering and the Professional Degree, Naval Engineer.

ABSTRACT

The S/N fatigue life gage is a device which resembles an ordinary metal foil strain gage. Its distinguishing characteristic is that its electrical resistivity increases as a function of the cumulative cyclic strain history of the material to which it is bonded. This gage was introduced in September, 1965, by its inventor, Mr. D. R. Harting, of the Boeing Company, Seattle, Washington. Currently it is being marketed on an experimental basis by Micro-Measurements, Inc., of Romulus, Michigan.

This thesis describes the results of several tests of the S/N gage which were conducted for the purpose of determining its possible use in certain engineering applications. These tests were performed at strain levels where many common structural materials fail after experiencing from 10,000 to 1,000,000 load cycles. Tests with zero mean load and various preloads were conducted in order to simulate loadings which actually occur in certain structures. All of the tests were made with a constant alternating load amplitude so as to provide a comparison with existing performance data of the gage.

The results of these tests show that the gage performance is nearly independent of mean load. Also the results show a good correlation with the tabulated performance characteristics of the gage. Included in this paper are some observations regarding the mechanics of the resistance change which occurs

in the gage and a proposal for mathematically relating the performance of the gage to other materials and modes of testing.

Thesis Supervisor: W. M. Murray

Title: Professor of Mechanical Engineering

in the light of a proposal for substantially reducing the expenditures of the State for other activities and would be

ACKNOWLEDGMENTS

I wish to express my appreciation to Professor W. M. Murray for initially suggesting this investigation as a thesis topic, and for his help and encouragement during its progress.

I am also indebted to Mr. D. R. Harting of the Boeing Company and to Mr. J. E. Stary of Micro-Measurements, Inc., for their kind cooperation.

And I wish to thank Mr. Ross Melton for his advice concerning the equipment used in conducting this investigation.

And, above all, I wish to thank my wife, Donna, for her patience and understanding and for doing all of the typing for me.

ATTENTION

I wish to express my appreciation to the
many of the faculty members who have
been helpful and the staff who have
been helpful.

I am most grateful to the
University of the South for the
many of the faculty members who have
been helpful.

And I wish to thank the
University of the South for the
many of the faculty members who have
been helpful.

And I wish to thank the
University of the South for the
many of the faculty members who have
been helpful.

TABLE OF CONTENTS

INDEX OF FIGURES.....	ii
SYMBOLS AND DEFINITIONS.....	iii
I. INTRODUCTION.....	1
II. OBJECTIVES.....	6
III. ANALYSIS OF THE S/W GAGE PERFORMANCE CHARACTERISTICS.....	8
IV. EXPERIMENTAL PROCEDURE.....	21
V. EXPERIMENTAL RESULTS.....	27
VI. DISCUSSION OF RESULTS.....	34
VII. CONCLUSIONS AND RECOMMENDATIONS.....	43
VIII. APPENDIX.....	50
A. Details of Preparing the Bending Specimen..	51
B. Description of Apparatus.....	53
C. Sample Calculations.....	63
D. Original Data.....	63
E. References.....	73

CONTENTS

11	LIST OF FIGURES.....	11
12	SYMBOLS AND ABBREVIATIONS.....	12
13	1. INTRODUCTION.....	13
14	2. OBJECTIVE.....	14
15	3. ANALYSIS OF THE DATA.....	15
16	4. EXPERIMENTAL PROCEDURE.....	16
17	5. EXPERIMENTAL RESULTS.....	17
18	6. DISCUSSION OF RESULTS.....	18
19	7. CONCLUSION AND RECOMMENDATIONS.....	19
20	8. REFERENCES.....	20
21	9. APPENDIX.....	21
22	10. DETAILS OF EXPERIMENTAL PROCEDURE.....	22
23	11. DESCRIPTION OF APPARATUS.....	23
24	12. SAMPLE CALCULATIONS.....	24
25	13. GRAPHICAL REPRESENTATION.....	25
26	14. SUMMARY.....	26

INDEX OF FIGURES

<u>FIGURE</u>		<u>Page</u>
I	TYPICAL S/N FATIGUE CURVE.....	2
II	S/N FATIGUE GAGE PERFORMANCE CURVES (#1).....	9
III	S/N FATIGUE GAGE PERFORMANCE CURVES (#2).....	10
IV	S/N FATIGUE GAGE PERFORMANCE CHARACTERISTICS.	12
V	PERFORMANCE MODULUS FOR S/N GAGE (CONSTANT STRAIN AMPLITUDE).....	16
VI	BENDING TEST SPECIMEN.....	23
VII (a)	RESISTANCE CHANGE AS A FUNCTION OF STRAIN FOR INITIAL FULL LOAD CYCLE - FIRST HALF CYCLE IN TENSION.....	29
VII (b)	RESISTANCE CHANGE AS A FUNCTION OF STRAIN FOR INITIAL FULL LOAD CYCLE - FIRST HALF CYCLE IN COMPRESSION.....	29(a)
VIII (a)	RESISTANCE CHANGE AT HALF CYCLE INTERVALS FOR THE FIRST TEN CYCLES - INITIAL HALF CYCLE IN TENSION.....	30
VIII (b)	RESISTANCE CHANGE AT HALF CYCLE INTERVALS FOR THE FIRST TEN CYCLES - INITIAL HALF CYCLE IN COMPRESSION.....	30
IX	RESULTS OF CYCLIC LOADING TESTS WITH ZERO PRELOAD.....	31
X	RESULTS OF CYCLIC LOADING TESTS WITH TENSILE PRELOAD.....	32
XI	RESULTS OF CYCLIC LOADING TESTS WITH COMPRESSIVE PRELOAD.....	33
XII	PERFORMANCE MODULUS FOR S/N GAGE AT CONSTANT STRESS AMPLITUDE ON 2024-T4 ALUMINUM.....	46
XIII	AF-1U FATIGUE MACHINE CALIBRATION CURVE FOR THE REVERSE BENDING FIXTURE.....	50

INDEX TO VOLUMES

Page	Volume
1	I
2	II
3	III
4	IV
5	V
6	VI
7	VII
8	VIII
9	IX
10	X
11	XI
12	XII
13	XIII
14	XIV
15	XV
16	XVI
17	XVII
18	XVIII
19	XIX
20	XX
21	XXI
22	XXII
23	XXIII
24	XXIV
25	XXV
26	XXVI
27	XXVII
28	XXVIII
29	XXIX
30	XXX

SYMBOLS AND DEFINITIONS

- n - Number of load cycles
- R - Total resistance of E/N gage (ohms)
- R_0 - Initial total resistance of E/N gage (ohms)
- ΔR - Increment of resistance change (ohms)
- ΔR - Total resistance change (ohms)
- $\bar{\epsilon}$ - Ratio of minimum strain to maximum strain
- σ - Stress (psi)
- $\mu\epsilon$ - Symbol for microstrain, or microinches per inch
- ϵ - Strain amplitude ($\mu\epsilon$)
- ϵ - Increment of strain ($\mu\epsilon$)
- ϵ_1 - Indicated strain ($\mu\epsilon$)
- ϵ_1 - Increment of indicated strain ($\mu\epsilon$)
- ϵ_m - Mean, or pre-load strain ($\mu\epsilon$)
- ϵ_o - Endurance limit strain of E/N gage ($\mu\epsilon$)
- ϵ_T - Total strain range ($\mu\epsilon$)

PROBATION REPORT

NAME: _____ DATE: _____

1. NAME OF PROBATIONER: _____

2. ADDRESS: _____

3. OCCUPATION: _____

4. DATE OF REPORT: _____

5. NAME OF PROBATION OFFICER: _____

6. DATE OF VISIT: _____

7. NAME OF PROBATIONER'S NEAREST RELATIVE: _____

8. NAME OF PROBATIONER'S NEAREST RELATIVE: _____

9. NAME OF PROBATIONER'S NEAREST RELATIVE: _____

10. NAME OF PROBATIONER'S NEAREST RELATIVE: _____

11. NAME OF PROBATIONER'S NEAREST RELATIVE: _____

12. NAME OF PROBATIONER'S NEAREST RELATIVE: _____

13. NAME OF PROBATIONER'S NEAREST RELATIVE: _____

14. NAME OF PROBATIONER'S NEAREST RELATIVE: _____

15. NAME OF PROBATIONER'S NEAREST RELATIVE: _____

16. NAME OF PROBATIONER'S NEAREST RELATIVE: _____

17. NAME OF PROBATIONER'S NEAREST RELATIVE: _____

18. NAME OF PROBATIONER'S NEAREST RELATIVE: _____

19. NAME OF PROBATIONER'S NEAREST RELATIVE: _____

20. NAME OF PROBATIONER'S NEAREST RELATIVE: _____

21. NAME OF PROBATIONER'S NEAREST RELATIVE: _____

22. NAME OF PROBATIONER'S NEAREST RELATIVE: _____

I. INTRODUCTION

In every practical design problem, the designer is faced with the choices of which structural material to use and what size to make each structural member. Many properties of the material may be considered before a final selection is made, but the physical strength of the selected material usually dictates the final dimensions of each member. Unfortunately for the designer, the statically determined strength properties, which are relatively easy to determine, may not be the best information upon which to base these important decisions.

Nearly every known material, when subjected to vibrating stresses, will eventually fail even though these stresses may be well within the material's statically determined strength limitations. There is, fortunately, a level of loading below which the likelihood of failure becomes very improbable. This boundary, called the endurance limit, provides an upper constraint for dynamic designing. It is analagous to the yield strength or ultimate strength criteria in static design and must not be exceeded if a virtually unlimited fatigue life for the member is desired.

Classically, the endurance limit of materials has been determined by counting the number of cycles to failure while subjecting a specimen of the material to alternating stresses

or strains of constant amplitude. Most of the common engineering metals have been tested and the results are well tabulated in handbooks. The customary graphical presentation employs the number of cycles to failure (n) as the abscissa and the stress amplitude (S) as the ordinate, resulting in a failure profile usually referred to as the S/N diagram. A typical S/N diagram is shown in Figure 1. In this diagram, S_1 represents the ultimate strength (failure at one-fourth of a cycle), whereas S_2 represents the endurance limit (stress below which failure becomes improbable).

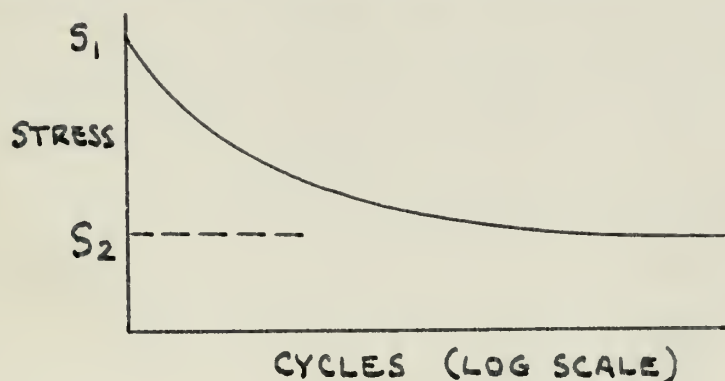
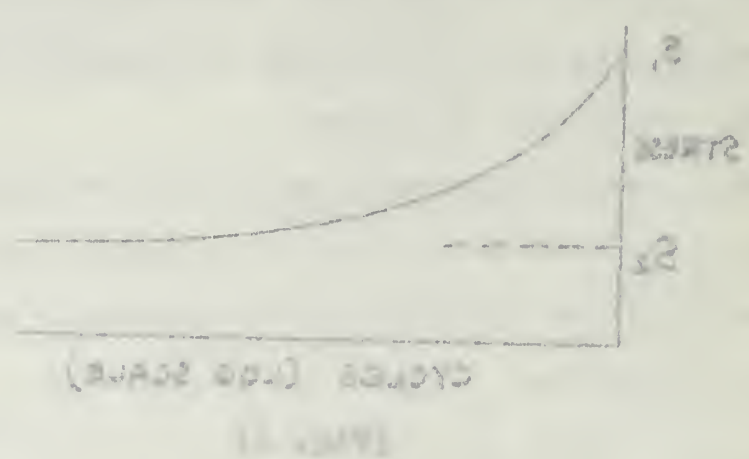


(Fig. 1)

The S/N diagram is useful in many respects as a means of presenting fatigue strength information. For example, it provides a graphic basis for comparing the effects of various factors which influence fatigue life. It is not very useful, however, in providing a means of predicting the fatigue life of a material when the loading is varied or of random amplitude. Cumulative fatigue damage is the term used when referring to the amount of a material's fatigue

It should be noted that the curve is not a straight line, but a curve which starts at the origin and increases at an increasing rate. This is due to the fact that the rate of change of the function is itself a function of the independent variable. The curve is concave up, which means that the slope of the tangent line to the curve at any point is increasing as the point moves along the curve. This is a characteristic of functions that are increasing at an increasing rate. The curve is also continuous and smooth, which means that it has no breaks or sharp corners. The curve is a good example of a function that is not linear, but which still has many of the properties of linear functions.



The curve is a good example of a function that is not linear, but which still has many of the properties of linear functions. It is continuous and smooth, and it has a unique tangent line at every point. The curve is also a good example of a function that is not one-to-one, as it fails the horizontal line test. This means that there are some horizontal lines that intersect the curve at more than one point. This is a characteristic of functions that are not strictly increasing or strictly decreasing. The curve is a good example of a function that is not invertible, as it does not have a unique inverse function. This is a characteristic of functions that are not one-to-one.

life which has been expended. More than one hundred theories have been advanced on this complicated subject, but the validity of each one is speculative because of the myriad of interacting variables involved. One of the principal difficulties encountered in relating theory and experimental results stem from the extensive scatter of data points inherent in fatigue testing. Relatively small factors exert a large influence when extended over thousands of load cycles. Another complication is that the definition of "failure" is not clearly established. As Bennitt (2) concludes, ultimate fracture is preceded by a crack initiation phase and a crack propagation phase, both of which are separate and distinct from one another. To summarize the problem, there is a need to reinforce the S/N diagram with reliable information in that blank region between the first load cycle and the point of ultimate failure so that the many individual influencing factors, including load changes, can be isolated and studied.

A possible means of indicating accumulative fatigue damage has been developed by Mr. D. M. Harting of the Boeing Aircraft Company and is presently marketed by William T. Bean, Inc. on an experimental basis. It is a small device called THE -S/N-* FATIGUE LIFE GAGE, which has the appearance of an ordinary strain gage. Strain gages are

*Trademark: Micro-Measurements, Inc., Rosulus, Michigan

designed and manufactured so as to minimize the effects of fatigue in the grid material. As a result, they are very accurate for measuring dynamic strains over a relatively short period of time, at the end of which time they fail quite suddenly. In contrast, the S/N gage functions as a rather poor dynamic strain gage which fails in a slow, measureable fashion. The grid of the gage is made from a material whose electrical conductivity changes as a result of cyclic straining. Also the backing is purposely made of very rigid material in order to carry the stresses around any point defects which may develop and thus prevent early failure in the grid due to cracking. When the gage is bonded to a structure whose fatigue life history is of interest, the electrical resistivity of the gage increases in an irreversible manner which is functionally dependent on both the strain level and the number of strain cycles. It performs at all times whether being continuously or periodically monitored by an indicating device. At the end of the structure's fatigue life, the total resistance change of the gage, depending upon the material to which it is attached, is of the order of ten per cent of the original gage resistance.

The S/N gage first became available in September, 1965. Because it is such a recent development, very little information concerning its performance in various applications has been published and much work must be done before its full potential can be realized. Determining and analyzing the

actual mechanism by which the resistivity changes is only one step in the development process. Its performance must be related to specific materials and the various types of loadings incurred in a particular application. Enough experimentation has been done, however, to indicate that the gage is potentially a very powerful tool in determining the effects of complicated loading histories on structural materials.

With machinery, vehicle, and building design becoming increasingly more sensitive to weight, the need for eliminating material which does not contribute to the overall strength becomes more and more important. When it eventually becomes possible to monitor cumulative fatigue damage, periodic replacing, refinishing, or redesigning of individual components can be more fully utilized as a means of minimizing weight. And with this new tool, designers may be able to exploit techniques which have previously been considered as too radical and uncertain for accepted practice.

II. OBJECTIVES

The central objectives of this investigation are as follows:

1. To perform an analysis of the S/N gage performance characteristics as determined and published by the manufacturer;
2. To relate the observed results of some experimental tests with the published performance characteristics of the gage.

In pursuing the first objective, the performance curves provided by the William T. Bean Corporation were used as a basis for the analysis. Since interpretation of the experimental results depends, in part, upon the analysis of these curves, and in order to preserve continuity in the development of certain ideas relating to these curves, the analysis is presented in its entirety as part III of this paper.

The experimental work was limited in scope to the following three categories of alternating strain amplitude:

- (a) $\pm 1500 \mu\epsilon$
- (b) $\pm 2000 \mu\epsilon$
- (c) $\pm 2500 \mu\epsilon$

At each of these levels of cyclic strain, static prestrains were superimposed to produce the following values of $\bar{\epsilon}$:

- (a) $\bar{\epsilon} = -1$

REV BEND

(b) $\bar{R} = 0$ TENSION ONLY

(c) $\bar{R} = -\infty$ COMPRESSION ONLY

\bar{R} is defined as the ratio $\frac{\text{minimum strain}}{\text{maximum strain}}$ and the standard sign convention is employed where (+) and (-) denote tension and compression respectively.

These particular values of strain and \bar{R} were chosen because they describe types and magnitudes of loading in a region of general interest. Many of the common alloys of iron, aluminum, copper, and nickel exhibit low cycle fatigue failure after experiencing from 10^4 to 10^6 load cycles under these conditions. This experimental work was also undertaken in order to pursue the following amplifying objectives:

1. To examine the effects of prestrain on the gage performance;
2. To examine the gage performance over the first few load cycles as a possible aid in explaining its behavior;
3. To examine the effects of different configurations of the electrical connections to the gage;
4. To obtain first-hand experience in using the gage so as to be more qualified in analyzing its performance.

(1) $\mathbb{R}^n \times \mathbb{R}^n \rightarrow \mathbb{R}^n$

(2) $\mathbb{R}^n \times \mathbb{R}^n \rightarrow \mathbb{R}^n$

It is known that the map $\mathbb{R}^n \times \mathbb{R}^n \rightarrow \mathbb{R}^n$ is surjective.

Let $\mathbb{R}^n \times \mathbb{R}^n \rightarrow \mathbb{R}^n$ be the map defined by $(x, y) \mapsto x + y$. Then the map is surjective.

Then the map $\mathbb{R}^n \times \mathbb{R}^n \rightarrow \mathbb{R}^n$ is surjective.

Let $\mathbb{R}^n \times \mathbb{R}^n \rightarrow \mathbb{R}^n$ be the map defined by $(x, y) \mapsto x + y$.

Let $\mathbb{R}^n \times \mathbb{R}^n \rightarrow \mathbb{R}^n$ be the map defined by $(x, y) \mapsto x + y$.

Let $\mathbb{R}^n \times \mathbb{R}^n \rightarrow \mathbb{R}^n$ be the map defined by $(x, y) \mapsto x + y$.

Let $\mathbb{R}^n \times \mathbb{R}^n \rightarrow \mathbb{R}^n$ be the map defined by $(x, y) \mapsto x + y$.

Let $\mathbb{R}^n \times \mathbb{R}^n \rightarrow \mathbb{R}^n$ be the map defined by $(x, y) \mapsto x + y$.

Let $\mathbb{R}^n \times \mathbb{R}^n \rightarrow \mathbb{R}^n$ be the map defined by $(x, y) \mapsto x + y$.

1. Let $\mathbb{R}^n \times \mathbb{R}^n \rightarrow \mathbb{R}^n$ be the map defined by $(x, y) \mapsto x + y$.

Let $\mathbb{R}^n \times \mathbb{R}^n \rightarrow \mathbb{R}^n$ be the map defined by $(x, y) \mapsto x + y$.

2. Let $\mathbb{R}^n \times \mathbb{R}^n \rightarrow \mathbb{R}^n$ be the map defined by $(x, y) \mapsto x + y$.

Let $\mathbb{R}^n \times \mathbb{R}^n \rightarrow \mathbb{R}^n$ be the map defined by $(x, y) \mapsto x + y$.

Let $\mathbb{R}^n \times \mathbb{R}^n \rightarrow \mathbb{R}^n$ be the map defined by $(x, y) \mapsto x + y$.

3. Let $\mathbb{R}^n \times \mathbb{R}^n \rightarrow \mathbb{R}^n$ be the map defined by $(x, y) \mapsto x + y$.

Let $\mathbb{R}^n \times \mathbb{R}^n \rightarrow \mathbb{R}^n$ be the map defined by $(x, y) \mapsto x + y$.

4. Let $\mathbb{R}^n \times \mathbb{R}^n \rightarrow \mathbb{R}^n$ be the map defined by $(x, y) \mapsto x + y$.

Let $\mathbb{R}^n \times \mathbb{R}^n \rightarrow \mathbb{R}^n$ be the map defined by $(x, y) \mapsto x + y$.

Let $\mathbb{R}^n \times \mathbb{R}^n \rightarrow \mathbb{R}^n$ be the map defined by $(x, y) \mapsto x + y$.

III. ANALYSIS OF THE S/N GAGE

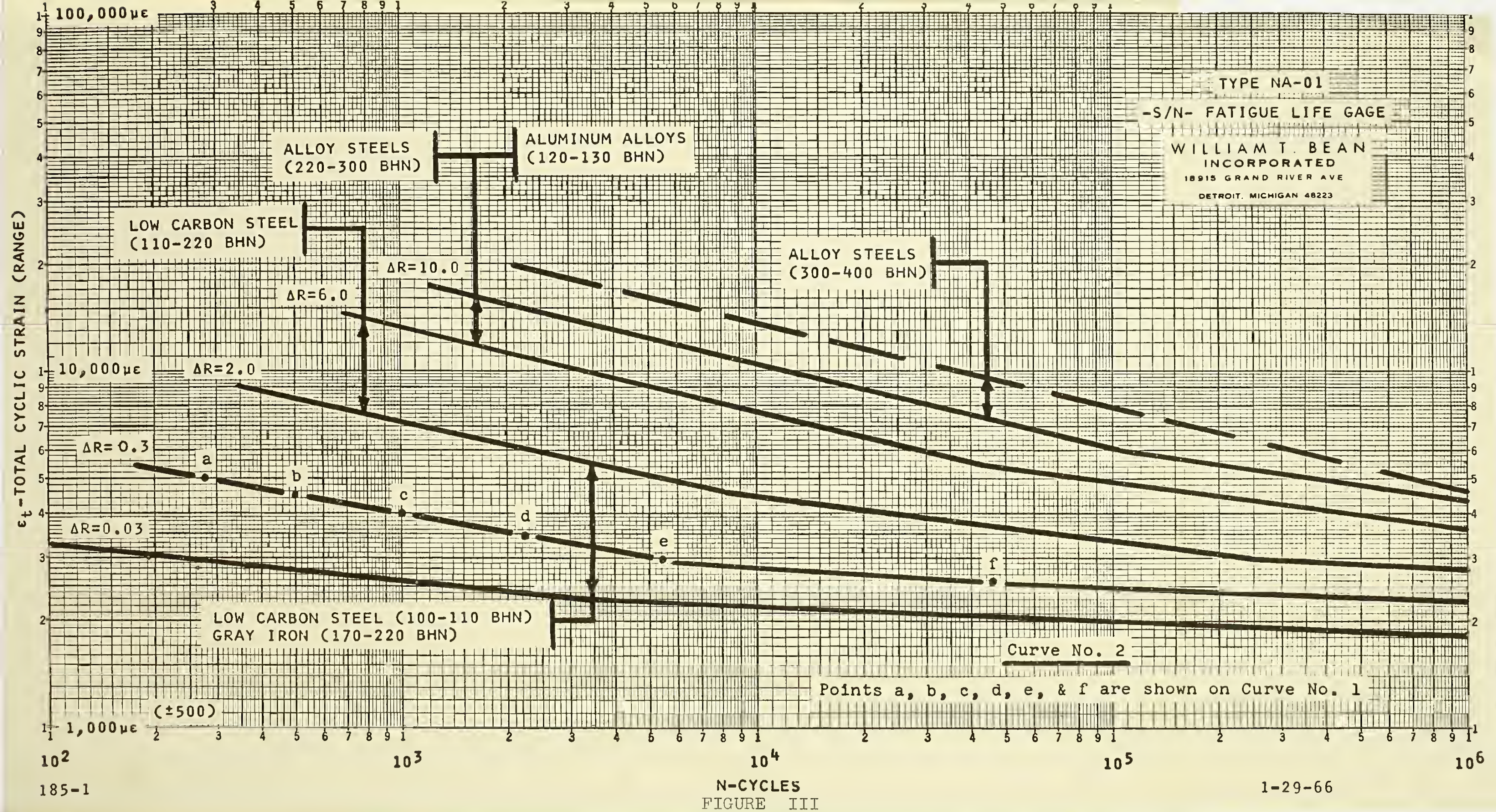
PERFORMANCE CHARACTERISTICS

The S/N gage performance curves shown in Figure II were provided by the William T. Bean Corporation. They are the results of a large number of tests in which the gage (Type BA-01) was mounted on various materials which include aluminums, stainless steels, cold rolled steels, fibre glass phenolic laminates, and epoxy castings. The method of testing was by means of a cantilever beam which was loaded in cyclic bending. Strain rather than stress was maintained at the same amplitude throughout each particular test. All of the gages were individually monitored and the averages of all the results are presented graphically in these curves.

An interesting variation of this plot where ΔR is treated as the parameter is shown in Figure III. It can be seen from this presentation that the lines of constant ΔR greatly resemble the failure lines on a typical fatigue diagram. This similarity, however, should only be considered in a general sense. Gross (4) has presented experimental evidence which indicates that the failure line for all steels nearly follows the relationship

$$\epsilon_T n^{0.34} = 0.17 \quad (1)$$

Superimposing a plot of this expression on Figure III reveals



that a cyclic strain which produces failure at 10^3 cycles results in a total resistance change of approximately 8 ohms. In contrast, a strain level which produces failure at 5×10^4 cycles results in a total change of only 4 ohms. It may be noted here that the units of ΔR may be expressed in either ohms or percentage of initial gage resistance. In either case, the numerical values are identical since the initial gage resistance has a value of 100 ohms.

In attempting to explore the uses of the S/N gage for measuring cumulative effects of non-uniform cyclic strains, a replotting of the performance curves was made which employed (n) as the parameter.* This presentation is shown in Figure IV. The idea behind this plot was that by having some knowledge of the number of load cycles experienced by the gage, the corresponding value of ΔR would provide an indication of the equivalent strain at which fatigue was induced in the structure. This, of course, is an engineering application which conceivably could provide an approach to correlating the gage's response in practical applications.

Two factors are immediately evident from this plot of ΔR versus ϵ on cartesian coordinates. They are:

*With regard to cumulative fatigue, the choice of (n) as a variable is unfortunate. Manson (10) discloses that the effects of strain hardening or softening as a result of changing the cyclic load intensity can greatly alter the fatigue life of a material exhibiting this tendency. The literature on fatigue theory, however, relies almost exclusively on this variable for want of a more descriptive one.

that a specific strain which produces failure at low values
 results in a total resistance increase of approximately 50%.
 In contrast, a strain level which produces failure at
 5 x 10⁶ cycles results in a total change of only 50%.
 It may be noted here that the ratio of 4.5 may be interpreted
 as either one of two things: (1) initial peak resistance, or
 (2) average, the numerical values are identical since the
 initial peak resistance was a value of 100,000.
 In attempting to explain the case of the 50% gain for
 increasing compressive stress of non-ferrous metal strains,
 a replotting of the experimental curves was made which indicated
 (a) as not pertinent. * This replotting is shown in Figure
 IV. The idea behind this plot was that of having some
 knowledge of the amount of load which was applied to the
 gauge, the corresponding value of ΔS would result in
 indication of the strain level at which failure occurred.
 Indeed in the diagram, this, in contrast to the replotting
 application which compressive load results in failure at
 increasing the gauge's resistance in direct proportion.
 The diagram was immediately evident from this plot of
 ΔS versus ϵ on various specimens, that the

*This strain is measured by the ratio of (1)
 to (2) as shown in the diagram. Figure (1) shows that the
 effect of stress is proportional to the ratio of (1) to (2)
 showing the ratio of (1) to (2) is directly proportional to
 the ratio of (1) to (2) as shown in the diagram. The
 diagram on Figure (1) shows the ratio of (1) to (2) is
 directly proportional to the ratio of (1) to (2) as shown in the diagram.

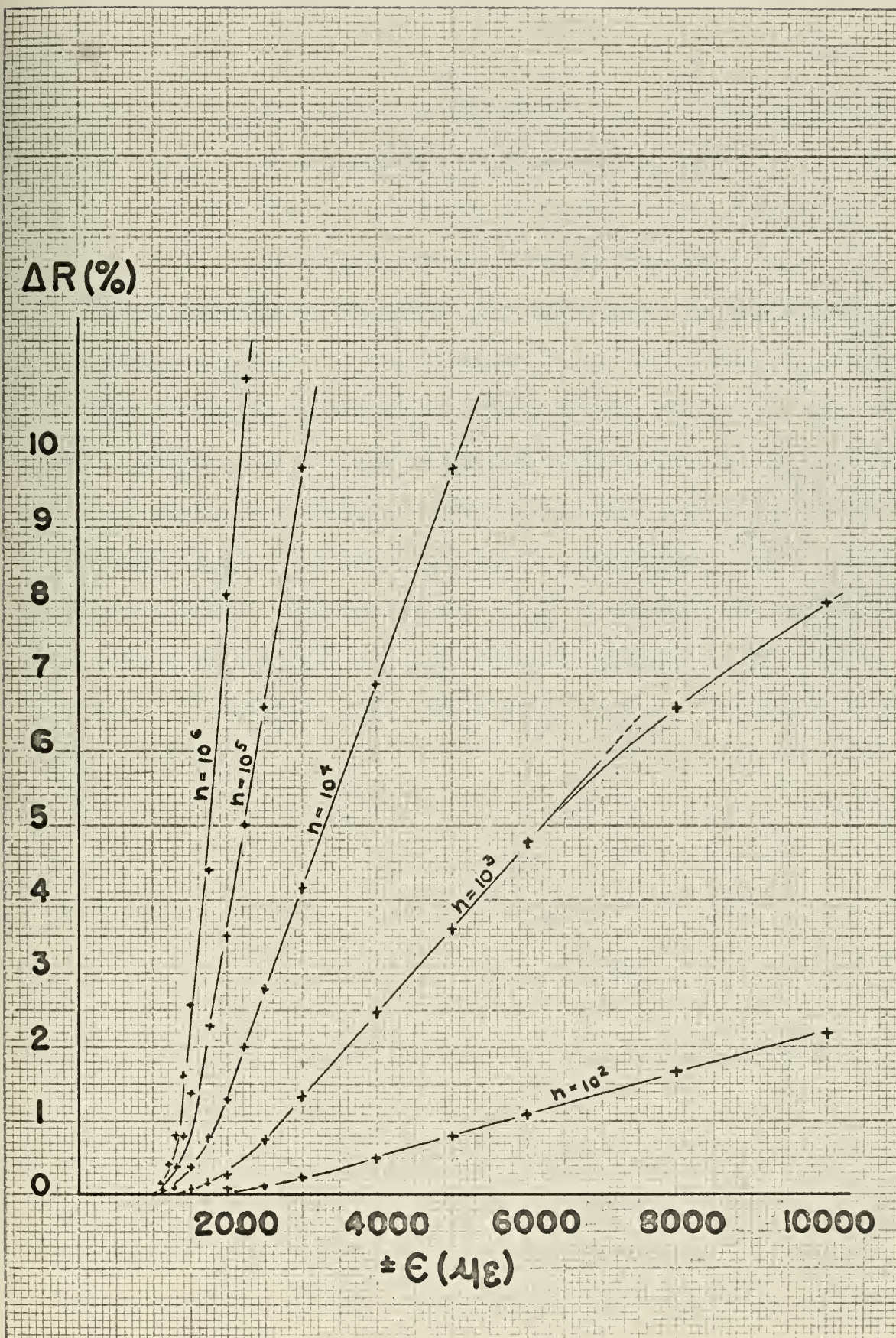


FIGURE IV

1. The lines of constant (n) can be very nearly approximated by straight lines;
2. The projections of these lines appear to intersect at a point on the abscissa.

These observations suggest that the slope of the lines of constant (n) is some function of (n). Furthermore, this slope can be interpreted as the partial derivative of ΔR with respect to ϵ , provided the derivative is qualified as representing the slope as determined by tests conducted at discrete values of constant strain amplitude. An initial crude plot of some values of $\left(\frac{\partial \Delta R}{\partial \epsilon}\right)$ versus (n) on log-log coordinates yielded an approximate straight line with a slope of roughly +0.33. This signifies a relationship of the form

$$\frac{\partial \Delta R}{\partial \epsilon} = K n^{0.33} \quad (2)$$

Integrating the above for ΔR produces the form

$$\Delta R = \int K n^{0.33} d\epsilon \quad (3)$$

where the partial differential is treated as a total differential by assuming that neither K nor (n) are explicit functions of ϵ . The intersection of the lines of constant (n) with the ϵ axis establishes a lower boundary condition which can be represented by the symbol ϵ_0 . Taking the above integral to the dummy variable upper limit of ϵ

produces the following relationship:

$$\Delta R = \int_{\epsilon_0}^{\epsilon} K n^{0.33} d\epsilon = (\epsilon - \epsilon_0) K n^{0.33} \quad (4)$$

This form is identical to that proposed by Harting (5), differing only in the numerical value of the exponent. ϵ_0 may be considered as an endurance limit, or a proportional limit of cyclic strain amplitude, since strains below this value have only second order effects on permanent resistance change. By the same argument, the term $(\epsilon - \epsilon_0)$ represents cyclic plastic strain, defined as that component of total cyclic strain which occurs beyond the limits of proportionality. Morrow (11) has presented very good arguments for basing fatigue theory on plastic strain energy.

With the above relationship derived, some attempts were made to determine the value of K for the actual performance curves of the S/N gage. As can be seen from Figure II, however, the performance at constant ϵ is not a straight line on log-log coordinates, but there is instead a 'hump' which occurs at different values of ΔR and (n) , depending upon the strain amplitude. This phenomenon renders the derived relationship incompatible as a continuous function.

By assuming that the ΔR function was probably valid only above the discontinuity, some further attempts were undertaken to arrive at a compatible relationship. This effort led to drawing a number of lines with a slope of 0.33

tangent to the upper curves. It was during this procedure that an observation was made which is rather obscured by the log-log presentation. This discontinuity in a line of constant strain amplitude can be removed by numerically adding a quantity to ΔR which is proportional to strain amplitude. Whether this constant is proportional to total strain or plastic strain is open to some questioning, but noting in Figure II that the lines for constant strain amplitudes less than $1400 \mu\epsilon$ are nearly straight and converging on log-log coordinates suggests that plastic strain is the influencing factor. Making this assumption, a relationship of the following form is indicated:

$$\Delta R = (\epsilon - \epsilon_0) [K_1 n^{K_2} - K_3] \quad (5)$$

A large scale replotting of Figure IV was made in order to accurately determine if a relationship of this form applies over a wide range of strains. The results, as shown graphically in Figure V, indicate that the relationship does in fact follow the above form over the entire range of (n) from 10^2 to 10^6 cycles. Determining the constants by trial and error resulted in the following approximate values for K_1 , K_2 , and K_3 :

$$\Delta R = (\epsilon - \epsilon_0) \left[(4.0 \times 10^{-4}) n^{0.246} - (10.0 \times 10^{-4}) \right] \quad (6)$$

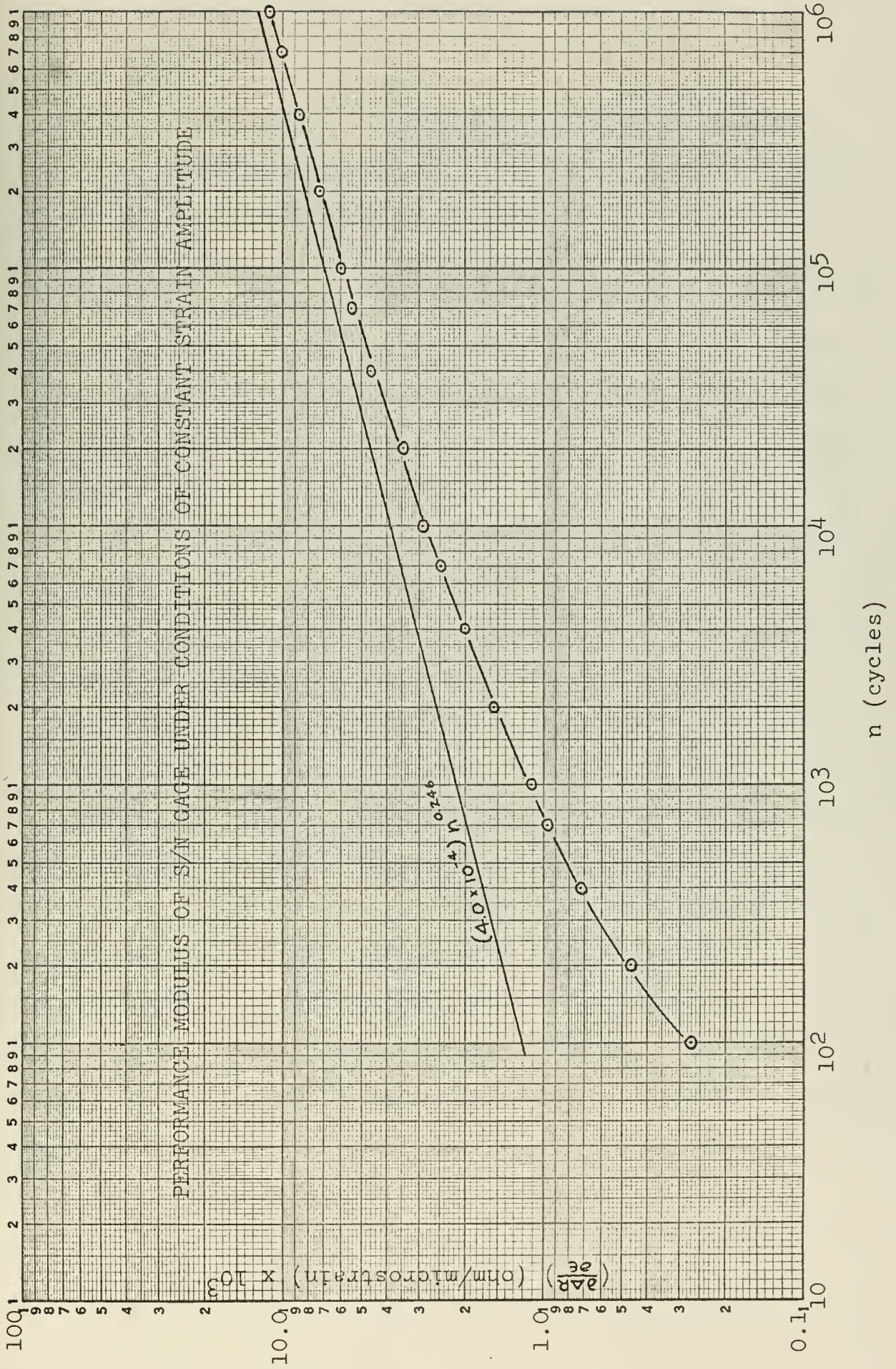


FIGURE V

TABLE I

GRAPHICALLY DETERMINED VALUES OF $\left(\frac{\partial \Delta R}{\partial \epsilon}\right)$ AND
 ϵ_0 INTERCEPT AS FUNCTION OF (π)

π (Cycles)	$\frac{\partial \Delta R}{\partial \epsilon} \left(\frac{\text{ohm}}{\mu\epsilon} \right)$	$\epsilon_0 (\mu\epsilon)$
1×10^2	$.29 \times 10^{-3}$	2200
2×10^2	$.47 \times 10^{-3}$	2100
4×10^2	$.72 \times 10^{-3}$	2000
7×10^2	$.98 \times 10^{-3}$	1900
1×10^3	1.11×10^{-3}	1850
2×10^3	1.54×10^{-3}	1700
4×10^3	2.00×10^{-3}	1550
7×10^3	2.50×10^{-3}	1500
1×10^4	2.89×10^{-3}	1520
2×10^4	3.43×10^{-3}	1400
4×10^4	4.62×10^{-3}	1450
7×10^4	5.45×10^{-3}	1500
1×10^5	6.00×10^{-3}	1350
2×10^5	7.25×10^{-3}	1350
4×10^5	8.79×10^{-3}	1350
7×10^5	10.00×10^{-3}	1300
1×10^6	11.30×10^{-3}	1200

TABLE I

THE $\left(\frac{\partial \Delta G}{\partial \epsilon}\right)$ OF VARIOUS ORIENTATIONS

(a) OF THE POLYMER IN THE LIQUID

θ	$\left(\frac{\partial \Delta G}{\partial \epsilon}\right)$	$\left(\frac{\partial \Delta G}{\partial \epsilon}\right)$
0°	$\epsilon \cos^2 \theta$	$\epsilon \cos^2 \theta$
10°	$\epsilon \cos^2 \theta$	$\epsilon \cos^2 \theta$
20°	$\epsilon \cos^2 \theta$	$\epsilon \cos^2 \theta$
30°	$\epsilon \cos^2 \theta$	$\epsilon \cos^2 \theta$
40°	$\epsilon \cos^2 \theta$	$\epsilon \cos^2 \theta$
50°	$\epsilon \cos^2 \theta$	$\epsilon \cos^2 \theta$
60°	$\epsilon \cos^2 \theta$	$\epsilon \cos^2 \theta$
70°	$\epsilon \cos^2 \theta$	$\epsilon \cos^2 \theta$
80°	$\epsilon \cos^2 \theta$	$\epsilon \cos^2 \theta$
90°	$\epsilon \cos^2 \theta$	$\epsilon \cos^2 \theta$
100°	$\epsilon \cos^2 \theta$	$\epsilon \cos^2 \theta$
110°	$\epsilon \cos^2 \theta$	$\epsilon \cos^2 \theta$
120°	$\epsilon \cos^2 \theta$	$\epsilon \cos^2 \theta$
130°	$\epsilon \cos^2 \theta$	$\epsilon \cos^2 \theta$
140°	$\epsilon \cos^2 \theta$	$\epsilon \cos^2 \theta$
150°	$\epsilon \cos^2 \theta$	$\epsilon \cos^2 \theta$
160°	$\epsilon \cos^2 \theta$	$\epsilon \cos^2 \theta$
170°	$\epsilon \cos^2 \theta$	$\epsilon \cos^2 \theta$
180°	$\epsilon \cos^2 \theta$	$\epsilon \cos^2 \theta$

Fitting this expression to the curves depends on the assumed value of ϵ_0 . Very good agreement was obtained by selecting values of ϵ_0 between 1300 and 1450 microinches per inch. As can be seen from Figure IV, the straight line projections of the constant (n) lines intersect the abscissa at slightly larger values of ϵ_0 for lower values of (n). A refinement to the expression for ΔR can be obtained by assuming that ϵ_0 is a weak function of the number of load cycles, as follows:

$$\epsilon_0 = 2500 n^{-0.047} \quad (7)$$

The actual lines of constant (n) do not really intersect the abscissa, but they become essentially tangent while converging on the origin. Since only the straight line portion of the constant (n) lines were used to derive the expression for ΔR , the expression is not accurate for values of ΔR less than approximately 0.3 ohms. Also the expression is not very accurate for high values of cyclic strains in the vicinity of (n) = 10^3 load cycles. It can be seen from Figure IV that the two points for 8000 $\mu\epsilon$ and 10,000 $\mu\epsilon$ do not fall on the straight line portion of the curve. For these high values of strain, the expression for ΔR becomes progressively less accurate beyond 200 load cycles.

Referring again to Figure V, which is the graphical representation of the bracketed term in equation (6), an

interesting analogy can be made regarding its physical meaning. It functions as a modulus which relates the plastic strain experienced by the gage to the resulting resistance change, much the same as Young's Modulus relates stress and strain. This curve must, of course, be qualified as the performance modulus at constant discreet values of cyclic strain amplitude. Rationalizing on this basis, it can be stated that the merits of this approach lie in the fact that, within the limits of accuracy with which the point values of $\left(\frac{\partial \Delta R}{\partial \epsilon}\right)$ were determined, the curve is smooth and continuous.

The only difference between equations (4) and (5) is the functional relationship between $\left(\frac{\partial \Delta R}{\partial \epsilon}\right)$ and (n) . In both cases, this relationship is parabolic in (n) , but in equation (5) the origin of the parabola is not at the initial load cycle. Equation (5) indicates that ΔR is a negative quantity during the first forty or so load cycles, which is obviously not true. This expression is only valid after approximately 100 load cycles when the transient effects of initial loading have presumably reached a steady state. The good agreement of equation (5) with the actual performance curves at least supports the validity of the assumed form of the relationship. If equation (5) is physically valid, then the following premises can be made:

1. Resistance change during the lifespan of the

is ($\frac{\partial R}{\partial \theta}$) the rate of change of R with respect to θ and

gage for a given cyclic strain amplitude can be expressed as the algebraic sum of two quantities; a "fatigue" component which is related to the number of load cycles, and a second component whose maximum value is independent of the number of load cycles.

2. The "fatigue" term is more nearly proportional to the fourth root of (n) rather than the cube root as first suspected. It may be noted that the curve of $\left(\frac{\partial \Delta R}{\partial \epsilon}\right)$ can be approximated over part of its range by a straight line with a slope of 0.33. At large values of (n) , $\left(\frac{\partial \Delta R}{\partial \epsilon}\right)$ values are difficult to determine accurately, but the slope of the curve appears to approach a value near 0.25.
3. The second component has a negative value. It represents the combined effects of all those factors which do not cause any further increase in ΔR once a certain value has been attained. This includes all of the transient effects in the initial cycles of loading.

By way of amplifying the third premise, it seems logical to assume that the gage will undergo some type of transient readjustment during its initial loading period. These readjustments could conceivably occur in the grid material,

but one cannot ignore such factors as the backing material, the adhesives which bond the grid to the backing and the backing to the specimen, and the possible relaxation of prestrains which may be induced in the gage during the manufacturing and mounting processes. Manson (10) has stated that cyclic strain hardening and softening, among other effects, manifests microstructural change and usually approaches saturation early in life.

IV. EXPERIMENTAL PROCEDURE

In order to pursue the objectives of this investigation with regard to the premises put forth in the analysis of the gage's performance characteristics, the following experimental tests were conducted:

1. Two gages were run through their initial load cycles while recording the resistance change at intervals during the cycle. In the first case, the initial half cycle was in tension followed by a half cycle in compression. In the latter case, this procedure was reversed.
2. These two gages were then run through nine more load cycles while recording the resistance change at the end of each half cycle.
3. Three specimens were tested with no prestrein while subjected to alternating loads which produced strain amplitudes of $\pm 1500 \mu\epsilon$, $\pm 2030 \mu\epsilon$, and $\pm 2490 \mu\epsilon$ respectively.
4. Three specimens were tested with static compressive prestrains of $1500 \mu\epsilon$, $2000 \mu\epsilon$, and $2500 \mu\epsilon$ while subjected to alternating loads which produced strain amplitudes of $\pm 1560 \mu\epsilon$, $\pm 1980 \mu\epsilon$, and $\pm 2510 \mu\epsilon$,

II. DISCUSSION

In order to study the properties of the interaction
with respect to the various and many in the field of the
paper's contribution, the following results
are given with comments.

1. The first part of the paper is devoted to the
study of the properties of the interaction with
respect to the various and many in the field of the
paper's contribution, the following results
are given with comments.

2. The second part of the paper is devoted to the
study of the properties of the interaction with
respect to the various and many in the field of the
paper's contribution, the following results
are given with comments.

3. The third part of the paper is devoted to the
study of the properties of the interaction with
respect to the various and many in the field of the
paper's contribution, the following results
are given with comments.

4. The fourth part of the paper is devoted to the
study of the properties of the interaction with
respect to the various and many in the field of the
paper's contribution, the following results
are given with comments.

5. The fifth part of the paper is devoted to the
study of the properties of the interaction with
respect to the various and many in the field of the
paper's contribution, the following results
are given with comments.

respectively.

5. Three specimens were tested with static tensile prestrains of $1500 \mu\epsilon$, $2000 \mu\epsilon$, and $2500 \mu\epsilon$ while subjected to alternating loads which produced strain amplitudes of $\pm 1560 \mu\epsilon$, $\pm 1980 \mu\epsilon$, and $\pm 2510 \mu\epsilon$ respectively.

A Sonntag SF-1U fatigue machine with reverse bending attachment was selected as the best available means of providing the cyclic loads required in testing the S/N gage. A detailed description of this equipment is found in Part B of the Appendix. Reverse bending was chosen because it afforded a means of testing two gages simultaneously under strains of identical magnitude but of opposite sense. By controlling the mean load so that its magnitude was the same as the amplitude of the alternating load, each side of the specimen was loaded exclusively in either tension or compression.

A standard fatigue specimen shape as shown in Figure VI was selected for the tests for several reasons. The extra width in the clamped portion causes lower localized strains in the vicinity of the clamp edges. This factor plus the narrower section near the center span of the specimen limits the region of highest failure probability to the center of the specimen. The tapered transition section provides a location for mounting the electrical terminal strips which

respectively.

3. These islands were found with the

latitude of 10° 45' N. and

longitude of 105° 45' E.

These islands were found with the

latitude of 10° 45' N. and

respectively.

A further 50-100 islands were found

attached and situated at the same distance of

providing the same shape as the 100 islands.

A detailed description of the islands is given in Part I

of the Appendix. Further details are given in Part II

of the Appendix. Further details are given in Part III

of the Appendix. Further details are given in Part IV

of the Appendix. Further details are given in Part V

of the Appendix. Further details are given in Part VI

of the Appendix. Further details are given in Part VII

of the Appendix.

A detailed list of islands is given in Part I

of the Appendix. Further details are given in Part II

of the Appendix. Further details are given in Part III

of the Appendix. Further details are given in Part IV

of the Appendix. Further details are given in Part V

of the Appendix. Further details are given in Part VI

of the Appendix. Further details are given in Part VII

of the Appendix. Further details are given in Part VIII

of the Appendix. Further details are given in Part IX

BENDING TEST SPECIMEN

Material: 2024-T4 Aluminum

Thickness: 0.1875 in.

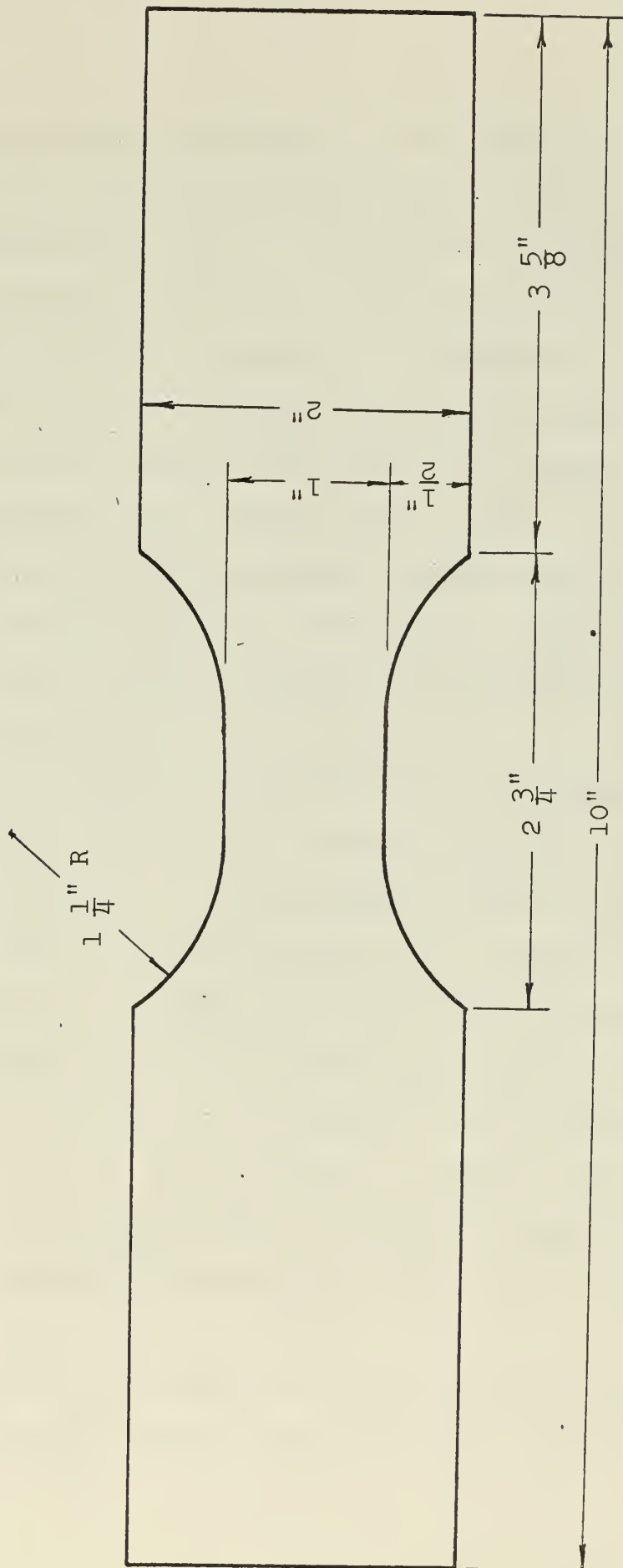


FIGURE VI

is subjected to less strain than is the center span.

All of the specimens were fabricated from 2" x 3/16" 2024 T-4 aluminum bar stock. This material was chosen because of its well-tabulated physical properties, its ease of fabrication, and its availability. Thickness of the material was selected in conjunction with the specimen dimensions so as to permit a wide range of loadings without producing excessive deflection in the specimen. Electrical limit switches on the SP-1U machine restrict the maximum bending deflection to ± 0.35 inches. All of the specimens were prepared and the gages mounted in a manner described in Part A of the Appendix.

Once the specimen was completed and the electrical connections installed, initial balanced readings of the strain and S/N gages were taken with the BAM-1 and BLH indicators. Both of these indicators are Wheatstone Bridge devices. In all the tests, one of the prepared specimens was used to provide the dummy ballast resistances necessary for electrically balancing the bridges. In addition to serving as a standard for comparing the resistances of all the specimen gages, this dummy specimen also provided temperature compensation for minor changes in ambient conditions.

The first step in conducting the cyclic testing was to install the reverse bending fixture with its proper tuning

is subjected to heat which may be the center area.

All of the specimens were subjected to a 1000

psi 10-15 aluminum bar shock. This material was chosen

because of its well-developed physical properties, its ease

of fabrication, and its availability. Thickness of the

material was selected in accordance with the existing

specimens so as to provide a wide range of loading stresses

producing extensive deformation in the specimens. (See Table)

These values are the 10-15 aluminum bar shock for the

loading values of 10, 15, 20, 30, 40, 50, 60, 70, 80, 90, 100

were produced and the values recorded in a report entitled

Part A of the Appendix.

Once the material was selected and the specimens

comparing finished, initial loading tests of the

specimens and the results were taken with the 1000-psi

inductance. This is shown in Table A of the Appendix.

Before the first test, one of the specimens was

used to provide the same loading conditions necessary

for electrically isolating the system. It consisted of

cutting a 1/2 inch thick aluminum bar specimen of all

the specimens given. This study was also made

temperature measurements for each specimen in which

it was

The first test in comparing the results of the

results of the first loading tests with the second loading

weights on the fatigue machine. Then the specimen was bolted in place between the bending fixture grips. Continuous strain gage readings were taken to insure that no misalignment within the bending fixture caused any axial force or unwanted bending moment. Small amounts of strain which were indicated after installation were easily removed by readjusting the preload mechanism of the machine.

With the specimen installed in the bending fixture and the dynamic strain indicating devices properly calibrated, the next step was to take and record the zero reference readings of the S/N gage resistance. This was done by means of a BLH Type N strain indicator which is described in Part B of the Appendix. All the readings for ΔR were taken with this instrument which measures resistance change in units of strain. The method of converting these readings into ΔR is discussed in Part C of the Appendix.

It was necessary with the SF-1U machine to be very careful when starting. Low modes of vibration are easily excited, which in turn produce unwanted overloading of the specimen.

The SF-1U is equipped with a counting device for determining the number of load cycles, but unfortunately it is run by a synchronous motor of its own and operates even when the eccentric load is not rotating. Furthermore, it is only accurate to within 1000 cycles. Therefore, the

number of cycles were determined on the basis of elapsed time rather than with a counter. Because the alternating load is applied at resonance, there is a clearly defined point, when bringing the machine up to speed, where the full value of cyclic loading begins. The reverse is true when stopping the machine. By simply multiplying elapsed time in minutes by 1800, the number of load cycles were computed very accurately.

Once the machine was up to speed, it was permitted to run undisturbed for a prescribed length of time. In the beginning of a test, the running intervals were of short duration, but as the experiment progressed and the resistance changed more slowly, the intervals were made longer. At each stopping point readings were taken and plotted on log-log coordinates for comparison with the curves in Figure II.

The foregoing procedure was used in all the tests with and without preload. At the beginning of each preloaded test, reference readings were taken with and without the preload applied. At subsequent stopping points two sets of readings were taken and referred to their respective initial readings. The results were identical. It can be concluded that resistance change may be measured at any point in the loading cycle provided such measurements are consistently taken at the same point each time.

V. EXPERIMENTAL RESULTS

The experimental results are presented graphically as follows:

- Figure VII (a) Resistance change as a function of strain for the initial full load cycle -- first half of cycle in tension.
- Figure VII (b) Resistance change as a function of strain for the initial load cycle -- first half cycle in compression.
- Figure VIII (a) Resistance change at half cycle intervals for $\pm 1500 \mu\epsilon$ cyclic strain -- initial half cycle in tension.
- Figure VIII (b) Resistance change at half cycle intervals for $\pm 2500 \mu\epsilon$ cyclic strains -- initial half cycle in compression.
- Figure IX Results of cyclic loading tests with zero preload.
- Figure X Results of cyclic loading tests with tensile preload.
- Figure XI Results of cyclic loading tests

V. CONCLUSIONS

The experimental results are discussed in the following

as follows:

Figure VII (a) Relationship between $\log k$ and $\log [M]$

Figure VII (b) Relationship between $\log k$ and $\log [M]$

Figure VII (c) Relationship between $\log k$ and $\log [M]$

Figure VII (d) Relationship between $\log k$ and $\log [M]$

Figure VII (e) Relationship between $\log k$ and $\log [M]$

Figure VII (f) Relationship between $\log k$ and $\log [M]$

Figure VII (g) Relationship between $\log k$ and $\log [M]$

Figure VII (h) Relationship between $\log k$ and $\log [M]$

Figure VII (i) Relationship between $\log k$ and $\log [M]$

Figure VII (j) Relationship between $\log k$ and $\log [M]$

Figure VII (k) Relationship between $\log k$ and $\log [M]$

Figure VII (l) Relationship between $\log k$ and $\log [M]$

Figure VII (m) Relationship between $\log k$ and $\log [M]$

Figure VII (n) Relationship between $\log k$ and $\log [M]$

Figure VII (o) Relationship between $\log k$ and $\log [M]$

Figure VII (p) Relationship between $\log k$ and $\log [M]$

Figure VII (q) Relationship between $\log k$ and $\log [M]$

Figure VII (r) Relationship between $\log k$ and $\log [M]$

Figure VII (s) Relationship between $\log k$ and $\log [M]$

Figure VII (t) Relationship between $\log k$ and $\log [M]$

with compressive preload.

The solid lines superimposed on Figures IX, X, and XI are the performance characteristics at particular values of strain amplitude taken from the curves in Figure II. They are included for reference purposes only.

and the following conditions:

1. The total area of the project shall be not less than 100 acres.
2. The project shall be located in a suitable area for the purpose of the project.
3. The project shall be approved by the local authorities.
4. The project shall be approved by the State Government.
5. The project shall be approved by the Union Government.

The project shall be approved by the Union Government.

The project shall be approved by the State Government.

The project shall be approved by the local authorities.

The project shall be approved by the Union Government.

The project shall be approved by the State Government.

The project shall be approved by the local authorities.

The project shall be approved by the Union Government.

The project shall be approved by the State Government.

The project shall be approved by the local authorities.

The project shall be approved by the Union Government.

The project shall be approved by the State Government.

The project shall be approved by the local authorities.

The project shall be approved by the Union Government.

The project shall be approved by the State Government.

The project shall be approved by the local authorities.

The project shall be approved by the Union Government.

The project shall be approved by the State Government.

The project shall be approved by the local authorities.

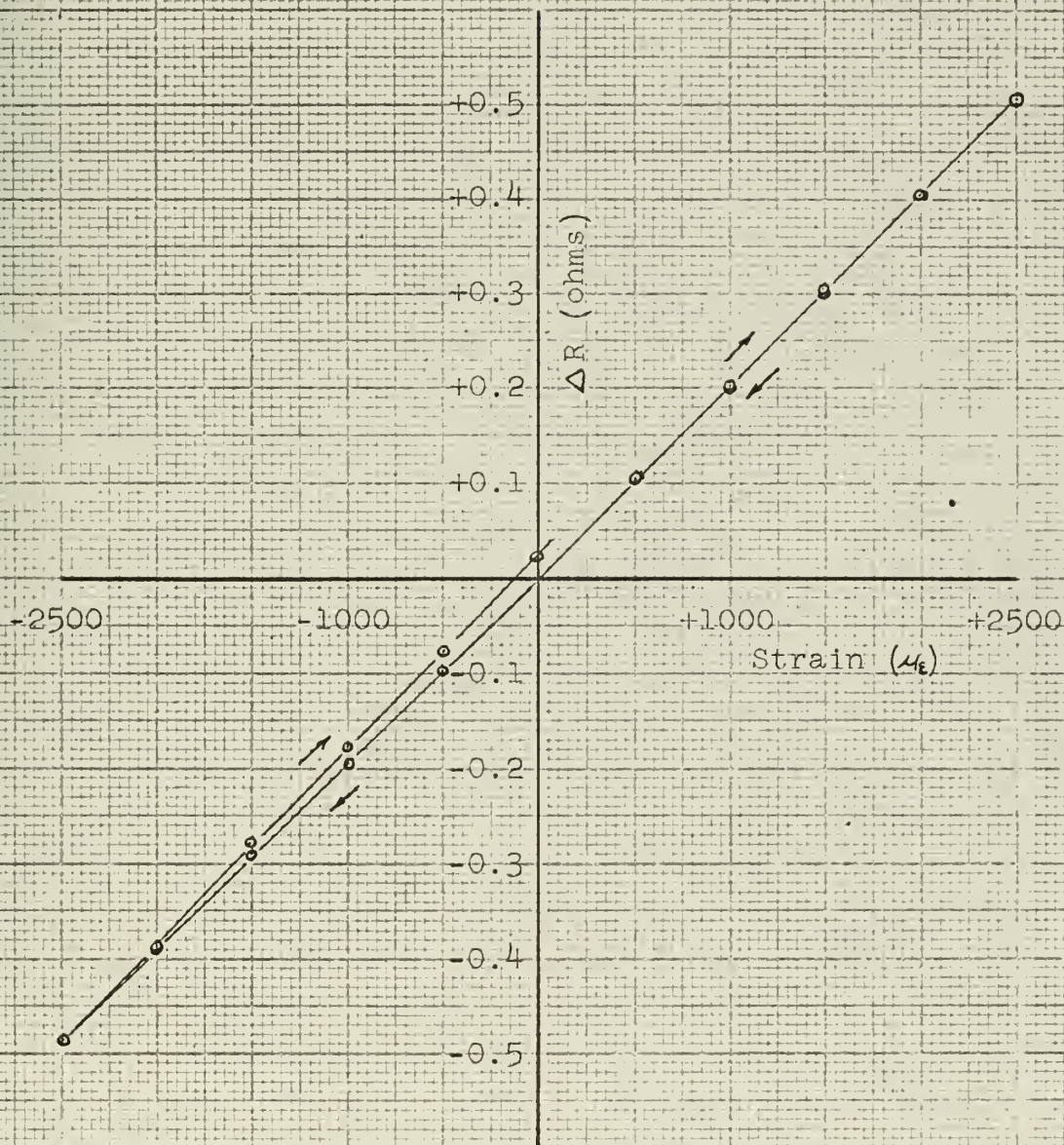
The project shall be approved by the Union Government.

The project shall be approved by the State Government.

The project shall be approved by the local authorities.

The project shall be approved by the Union Government.

FIGURE VII (a)

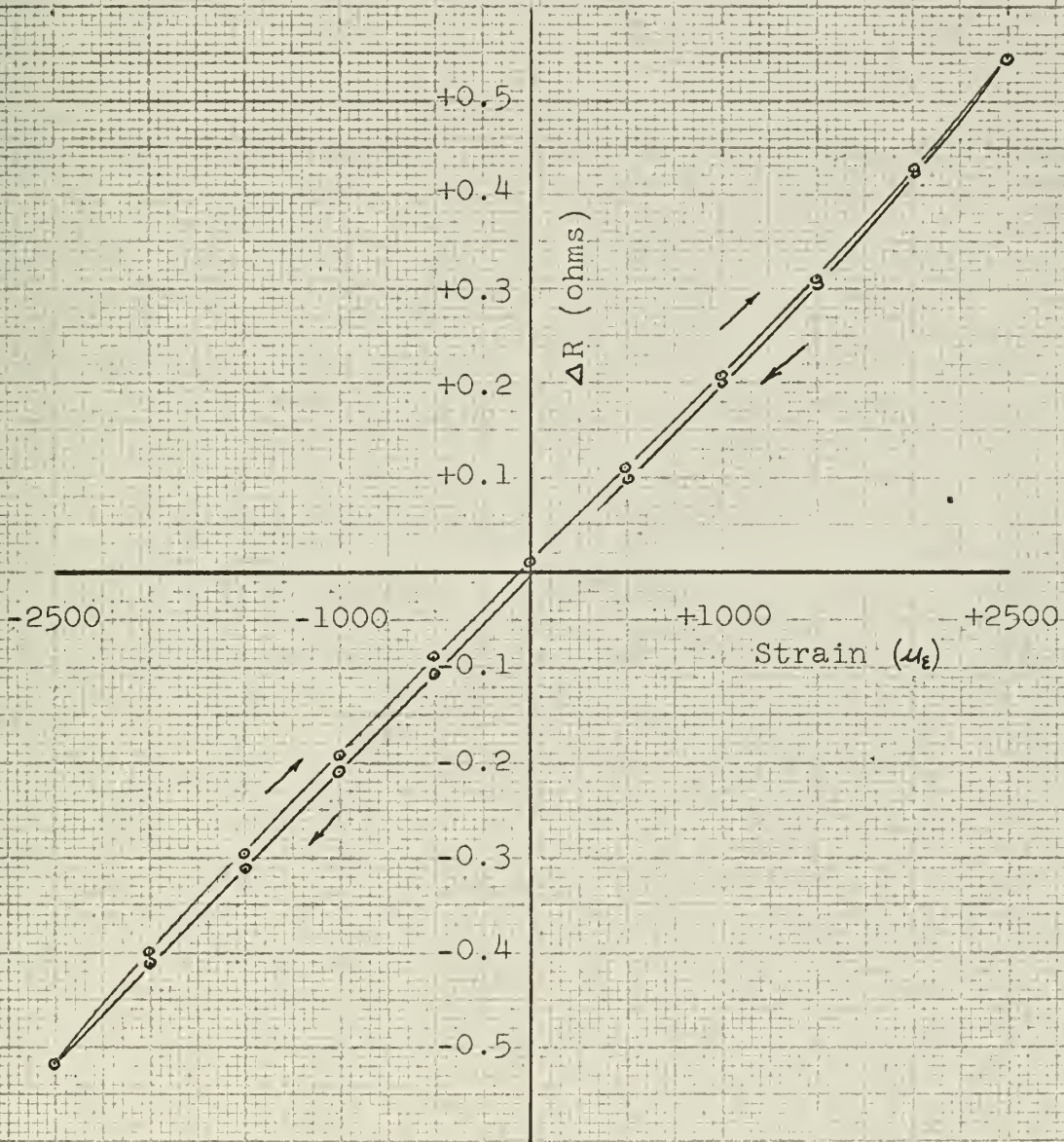


RESISTANCE CHANGE AS A FUNCTION OF STRAIN FOR

INITIAL FULL LOAD CYCLE

FIRST HALF CYCLE IN TENSION

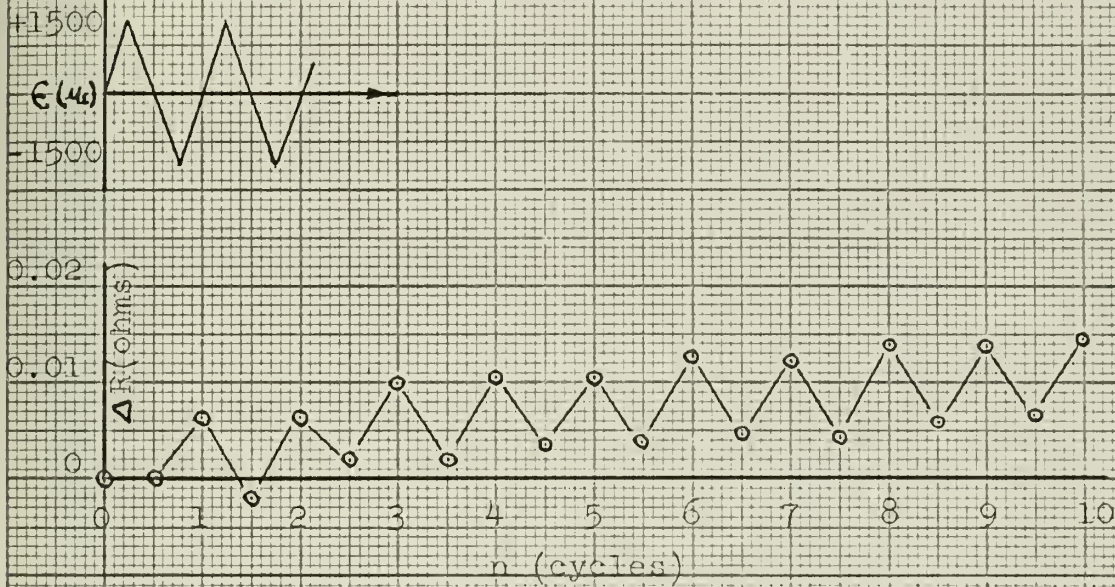
FIGURE VII (b)



RESISTANCE CHANGE AS A FUNCTION OF STRAIN FOR
INITIAL FULL LOAD CYCLE

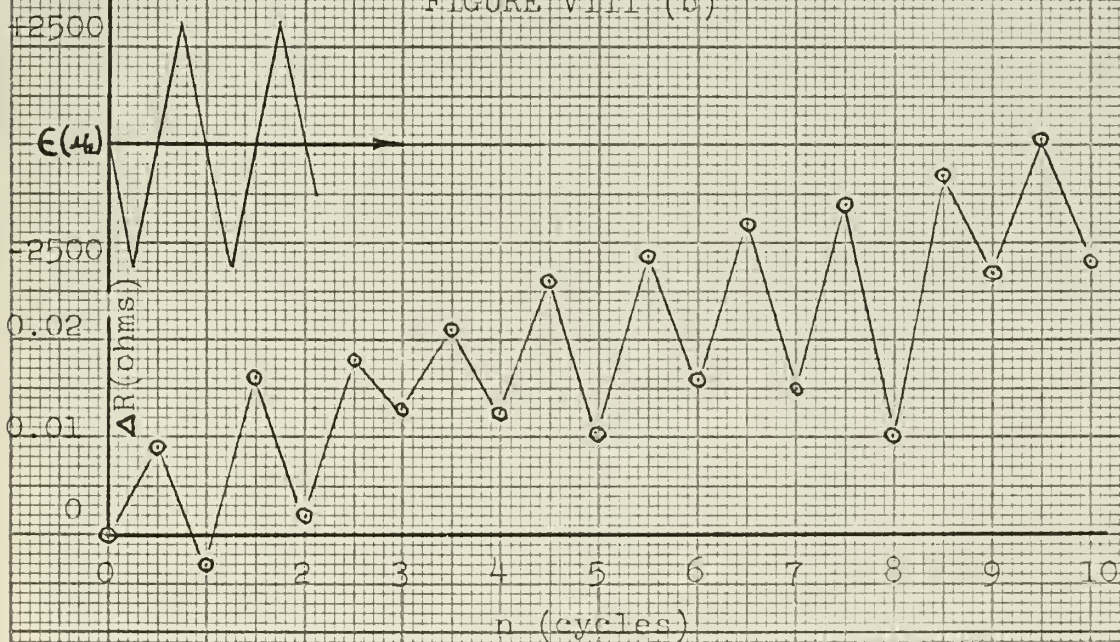
FIRST HALF CYCLE IN COMPRESSION

FIGURE VIII (a)



RESISTANCE CHANGE AT HALF CYCLE INTERVALS
FOR THE FIRST TEN CYCLES
FIRST HALF CYCLE IN TENSION

FIGURE VIII (b)



RESISTANCE CHANGE AT HALF CYCLE INTERVALS
FOR THE FIRST TEN CYCLES
FIRST HALF CYCLE IN COMPRESSION

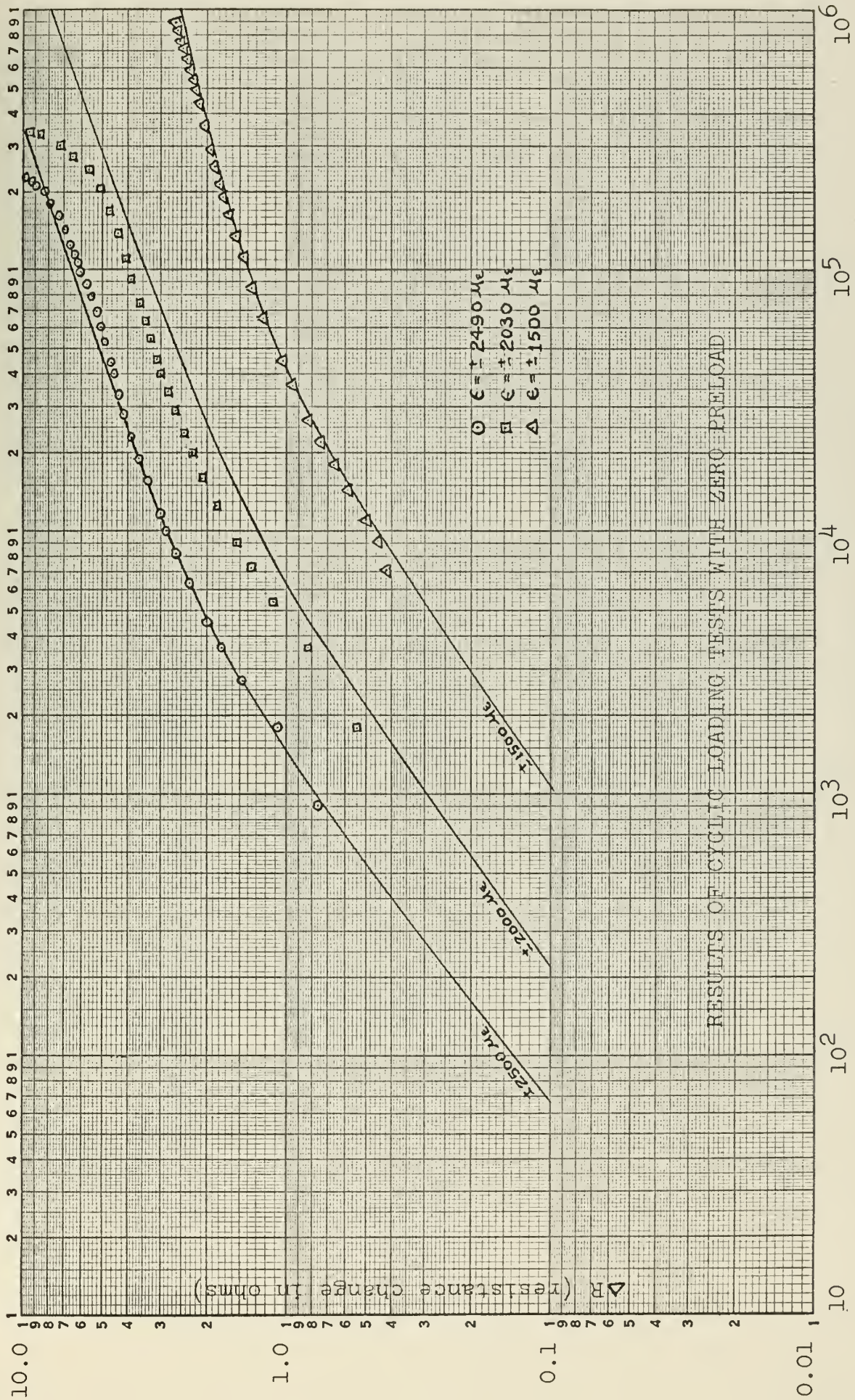
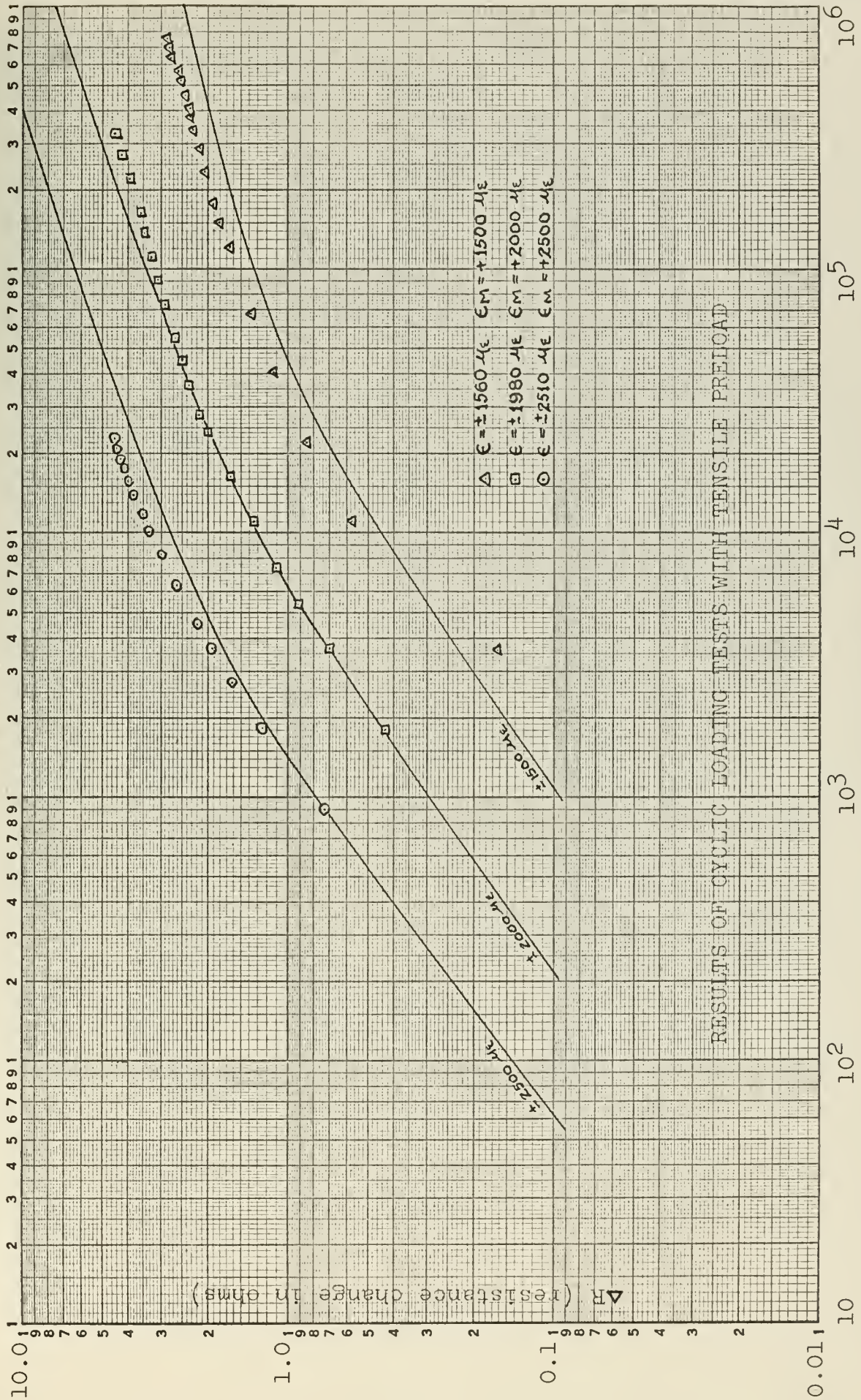


FIGURE IX



n (cycles)

FIGURE X

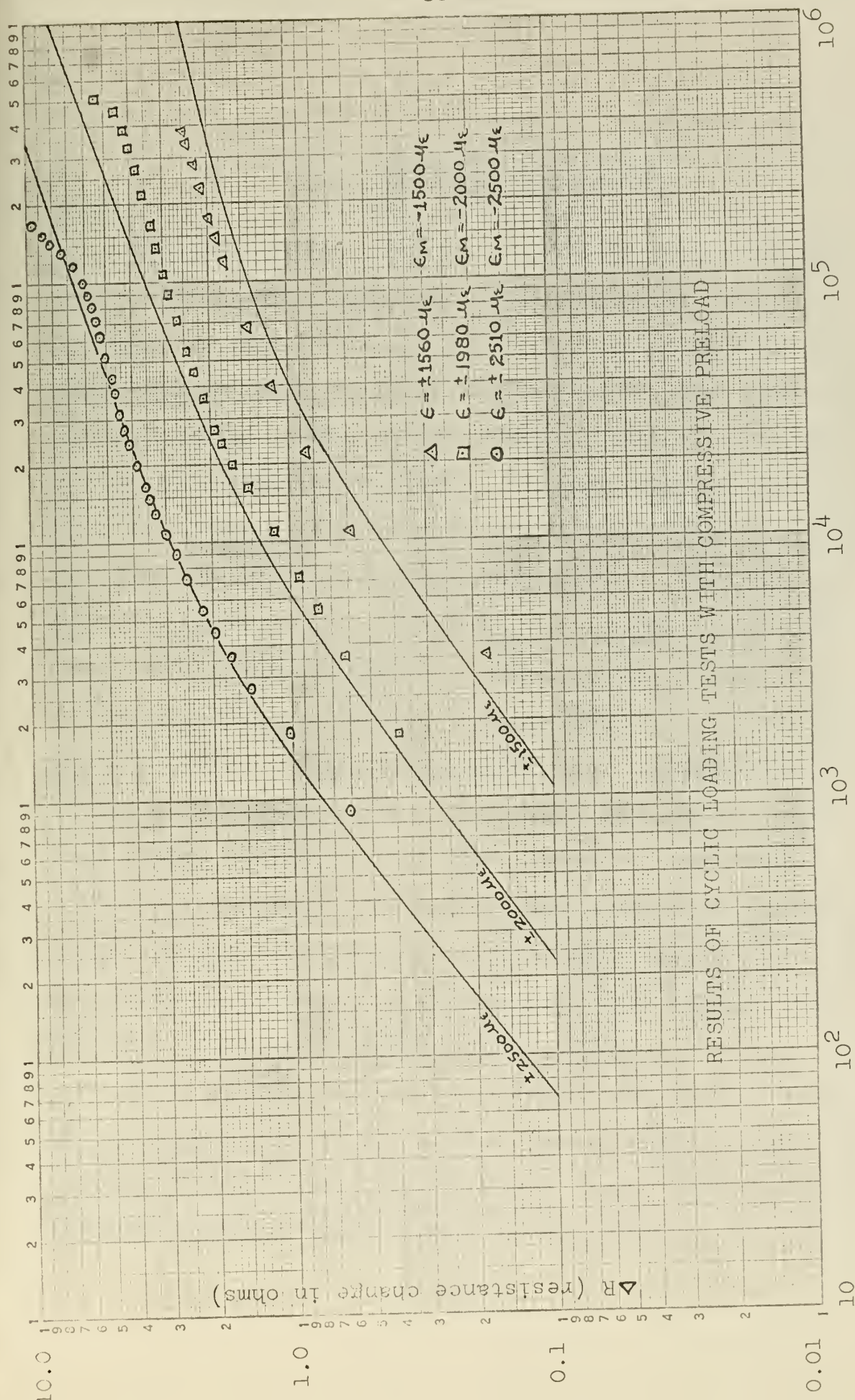


FIGURE XI

VI. DISCUSSION OF RESULTS

The experimental results are entirely dependent upon the accuracy with which cyclic and mean strains were determined. All of the strain gages which were used were certified by their manufacturer as having a gage factor of 2.095 ± 0.5 per cent, and the static strain readings are within this order of accuracy. In measuring the cyclic strains, however, a compound error resulted from using an oscilloscope to display the strain signal. The scope can be read, at best, to within $\pm 20 \mu\epsilon$ at the peak-to-peak values which were encountered. This source of error influenced both the initial scope calibration and the final reading. Reported cyclic amplitudes are believed to be accurate to within 1.5 per cent to 2.0 per cent of their true value. It was not possible to monitor the strains throughout an entire test because the gages have a comparatively short life at the amplitudes used in these experiments. In the tests at $\pm 1500 \mu\epsilon$, for example, gage failure was observed after approximately 20,000 cycles.

By using strain gages to determine the cyclic loads, it was not necessary to rely on the load settings of the SF-1U machine for accuracy. Nevertheless, it was advantageous to perform a precise calibration of the machine in the mode of

VI. DISCUSSION OF RESULTS

The experimental results are presented in the following tables.

The accuracy with which the results were

determined. All of the data were obtained with

certified by their manufacturers as having a true length of

2.000 ± 0.0005 per cent, and the results given in the tables are

within this order of accuracy. In measuring the length

of the rods, however, a constant error resulted from using the

calipers to bring the rods to the same length. The error was

found to be at best, ± 0.0005 per cent, and the results given

values which were determined. This amount of error

influenced both the length and the weight of the rods.

Reading. The results given in the tables are believed to be

correct to within ± 0.0005 per cent, and the results of the

first value. It was not possible to measure the length

throughout the entire length of the rods and a comparison

of the results with the results of the other measurements.

The results are ± 0.0005 per cent, and the results are

correct to within approximately ± 0.0005 per cent.

By using these data to determine the length of the rods, it

was not necessary to use the same method as was used in the

measure for density. In determining the density, it was necessary to

perform a series of measurements of the length of the rods at

testing which was employed so that the settings at the start of each test could be as close as possible to those desired. Changing the load settings during a test is extremely undesirable at this point in the development of the S/N gage since insufficient information exists as to the effects of such a change. The load setting calibration, which is shown graphically in Part A of the Appendix, provided a means of cross checking the accuracy of each strain measurement. In addition, it served to expose an inaccuracy in the SF-1U machine since all the observed strains were approximately 125 per cent greater than they should have been for a particular setting. This finding is noted in passing because it serves to illustrate a very important point with regard to fatigue testing in general. Most testing is done without the use of strain indicating equipment, which means that such a discrepancy would probably be attributed to some other factor when interpreting the results.

Measurements of ΔR with the BLH indicator were extremely accurate. In a laboratory test of this device using decade resistance boxes, the variation of measured resistance change over a total range of 8 ohms was less than 0.01 ohm. Lead wire and terminal strip resistances in the gage circuitry were found to be less than 0.02 ohm, and since this quantity is incorporated in the initial gage resistance of 100 ± 0.2 ohms when computing ΔR , their effects are

considered negligible.

The plot of S/N gage performance shown in Figure VII (a) serves to illustrate a point which has been suggested by the gage's manufacturer. If the first half cycle of loading is in tension, the resistance change is linear with respect to strain, thereby making the gage usable for measuring strain under these constraints. This feature can be used to verify the strain field at the beginning of a test. The gage factor, which is the ratio of percentage resistance change to induced strain, has a numerical value of 2.04 in this application. It can be seen in Figure VII (b) that the above relationship does not hold true once the gage has been cycled in compression. Figures (a) and (b) both show that the gage is noticeably affected by the compressive half cycle.

Figure VIII (a) and (b) are the results of slowly cycling two specimens in reverse bending by using the preload mechanism of the SF-1U fatigue machine. These results are included to illustrate that the resistance changes experienced by the gage during its initial loading cycles are not only a function of the magnitude and number of strain cycles, but also depend on whether the half cycle is in compression or tension. It can be seen from these plots that the gage experiences an increase in resistance during a compressive half cycle, and also that there is a

THE COURT OF APPEALS IN THE DISTRICT OF COLUMBIA, in its decision in *United States v. Galt*, 401 F.2d 1008 (D.C. Cir. 1968), cert. denied, 394 U.S. 970 (1969), has held that the government's failure to disclose the existence of a confidential source to the defense in a criminal case is a violation of the defendant's right to a fair trial. The court in *Galt* stated that the government's failure to disclose the existence of a confidential source to the defense is a violation of the defendant's right to a fair trial because the defense is entitled to know the identity of the confidential source in order to cross-examine the source and to impeach the source's testimony. The court in *Galt* also stated that the government's failure to disclose the existence of a confidential source to the defense is a violation of the defendant's right to a fair trial because the defense is entitled to know the identity of the confidential source in order to cross-examine the source and to impeach the source's testimony. The court in *Galt* also stated that the government's failure to disclose the existence of a confidential source to the defense is a violation of the defendant's right to a fair trial because the defense is entitled to know the identity of the confidential source in order to cross-examine the source and to impeach the source's testimony.

partial recovery from this change during the tensile half cycle. These observations suggest that the gage goes through a period of adjustment to conditions of cyclic straining during its initial cycles of loading.

Figure IX shows the results of the tests in cyclic loading with no preload.* The test at $\pm 1500 \mu\epsilon$ produced results nearly identical to those in Figure II. At 872,000 cycles, the resistance was only 0.15 ohm higher than anticipated, or, in terms of total resistance change, greater by approximately 6 per cent. It is interesting to note that the curve for $\pm 1500 \mu\epsilon$ in Figure II shows significant revision from previously published performance curves at this strain level. The experimental results in Figure IX are in better agreement with this latest revision.

The test results at $\pm 2490 \mu\epsilon$ show even better agreement, differing by less than 4 per cent out to approximately 200,000 load cycles. Beyond this point, the resistance increased much more rapidly than expected due to the formation of a small blister beneath the gage. This blister was the result of the adhesive parting from the aluminum. No cracking of the specimen was observed in this region.

*Comparison of all the experimental results with the performance curve in Figure II is somewhat inexact because of the width of the lines used in the latter to portray the gage's performance. This factor becomes quite significant in the log-log presentation, where the width of a line can account for as much as 0.5 ohm at higher values of ΔR .

The test at $\pm 2030 \mu\epsilon$ produced resistance change approximately 10 per cent greater than expected. This test was run with a weight setting which should have produced an alternating strain of $\pm 1990 \mu\epsilon$, but there was misalignment of the specimen in the bending fixture which was not detected by static strain measurements. Because the bearings of the bending fixture were not perfectly parallel, a small amount of bending was produced about an axis perpendicular to the specimen each time it was deflected by the load. This condition was first indicated by the dynamic strain readings and later confirmed visually, but the test was completed without making any changes. The results were affected in this test because the S/N gage and the strain gage were mounted on the same side of the specimen on opposite sides of the centerline. If the S/N gage had been mounted on the centerline, this misalignment would have had no noticeable consequences.

After approximately 250,000 load cycles, the resistance of the gage being cycled at $\pm 2030 \mu\epsilon$ began to increase more rapidly than predicted. This increase took place gradually over the following 100,000 load cycles until the resistance had changed a total of 10 ohms, at which time the test was terminated. Following removal of the gage from the specimen, it was discovered that the adhesive had broken away from the aluminum over a very small area under the grid.

The case at 2091 (Graham) involved a large
community in the area of the river. This case
was not a simple matter and it was not
settled until 1950. The case was settled
and the settlement in the amount of \$100,000 was
settled by a large community. The case was settled
and the settlement was not a simple matter. The
settlement was not a simple matter and it was not
settled until 1950. The case was settled and the
settlement was not a simple matter. The settlement
was not a simple matter and it was not settled
until 1950. The case was settled and the settlement
was not a simple matter. The settlement was not a
simple matter and it was not settled until 1950.

No cracking was visible in this area.

The tests in which 1500 $\mu\epsilon$ of preload was superimposed on an alternating strain of $\pm 1560 \mu\epsilon$ produced results which were nearly identical in both the compression and the tension gages. Interpolation shows that the data points also followed the performance characteristics in Figure II very closely. Resistance change for the compression gage was 0.13 ohm greater than the tension gage at 372,000 cycles, at which time the compression test was terminated because of a broken lead connection on the gage. To what extent this weakened connection influenced the gage's performance is unknown. The tension gage was tested to 722,000 cycles without showing any noticeable deviation from the performance curves in Figure II.

The test in which 2000 $\mu\epsilon$ of preload was superimposed on an alternating strain of $\pm 1980 \mu\epsilon$ produced results in which the resistance change of the tension gage was consistently greater than the compression gage by a factor of approximately 14 per cent. The tension gage followed the performance curves for no preload out to 50,000 cycles, at which time the data points began to fall progressively farther below the curve. The compression gage followed this same pattern of behavior. At approximately 325,000 cycles, the tension gage failed quite suddenly, after which it can be seen that the resistance of the compression gage began to

The results of the 1950-51 survey are summarized in an accompanying table at p. 1000. The results of the 1950-51 survey are summarized in an accompanying table at p. 1000. The results of the 1950-51 survey are summarized in an accompanying table at p. 1000.

increase more rapidly. Very shortly after the last reading was taken at 506,000 cycles, the specimen fractured. Observations of the fracture lines and the location of the fracture indicate that the crack initiated directly under the tension gage. This would explain the sequence of events following failure of the tension gage.

The tests in which 2500 $\mu\epsilon$ of preload was superimposed on an alternating strain of $\pm 2510 \mu\epsilon$ were, unfortunately, not run concurrently. The tension gage on the original specimen failed during the initial loading cycles when the adhesive broke away from the aluminum. An additional specimen was tested in which the bonding surface was intentionally made rougher to facilitate better adhesion, but even this test failed for the same reason after 23,000 load cycles. The results which were obtained are included in the graphical presentation because they illustrate that the resistance change was within 10 per cent of the curve in Figure II. No failure in the adhesive bonding of this second specimen was apparent until after the last reported resistance reading.

The compression gage was tested successfully, giving results which were nearly identical to the curve in Figure II out to 50,000 cycles. At this point, the data falls progressively farther below the curve as did tests at lower strain levels. After 100,000 cycles, the resistance started

because more rapidly. Very slowly after the first reading

was taken at 30,000 cycles, the machine continued.

Observations of the frequency lines and the intensity of the

frequency bands show the same intensity at all

the reading points. This would indicate the absence of any

frequency change in the reading range.

The tests in which the machine was used as a frequency

as an indicating device at 20,000 and 30,000 cycles, respectively,

and the results are as follows:

Machine failed during the tests, leaving only the

machine parts from the machine. In addition,

machine was tested in which the machine was

extensively used in which the machine was

has been this test failed for the same reason as the

last test. The results show that the machine was

in the frequency range of 20,000 to 30,000 cycles.

The machine shows no change in the test of the

machine. In the machine the machine was

tested and the results were as follows:

Machine failed.

The machine was tested in which the machine was

tested and the results were as follows:

Machine failed. In the machine the machine was

tested and the results were as follows:

Machine failed. In the machine the machine was

to increase until fracture occurred at 220,000 cycles. This is believed to be due to crack initiation on the other side of the specimen since there was no visible indication of adhesive problems.

In part III of this paper, it was shown that the endurance limit of the gage was approximately $\pm 1350 \mu\epsilon$. By virtue of this property, errors in determining strain amplitudes are not directly relatable to the resulting errors in ΔR . In the range of these tests, an error of 1 per cent in measuring strain will result in a resistance change error of approximately 3 per cent. Therefore, errors of as much as 6 per cent in ΔR are within the order of testing accuracy.

All of the test results shown in Figures IX, X, and XI exhibit generally good agreement with the curves from Figure II. It must be recalled, however, that the experimental results, which were produced under conditions of constant cyclic stress amplitude, are compared with the results of tests performed under conditions of constant strain amplitude. The principal difference between these two modes of testing is that the constant strain tests are not affected by changes in strength properties of the specimen which occur as a result of cyclic bending. It can be seen from Figures IX, X, and XI that the data points all describe curves which are nearly parallel in log-log coordinates, indicating that the

[illegible]

effects of minor changes in the specimen properties were uniform and proportional to strain amplitude over the range of testing.

effects of these changes in the system properties are
 analyzed and reported for the whole system over the time
 of testing.

The system is tested by the following procedure:

1. The system is tested by the following procedure:

2. The system is tested by the following procedure:

3. The system is tested by the following procedure:

4. The system is tested by the following procedure:

5. The system is tested by the following procedure:

6. The system is tested by the following procedure:

7. The system is tested by the following procedure:

8. The system is tested by the following procedure:

9. The system is tested by the following procedure:

10. The system is tested by the following procedure:

11. The system is tested by the following procedure:

12. The system is tested by the following procedure:

13. The system is tested by the following procedure:

14. The system is tested by the following procedure:

15. The system is tested by the following procedure:

16. The system is tested by the following procedure:

17. The system is tested by the following procedure:

18. The system is tested by the following procedure:

19. The system is tested by the following procedure:

20. The system is tested by the following procedure:

21. The system is tested by the following procedure:

VII. CONCLUSIONS AND RECOMMENDATIONS

The most obvious conclusion which can be drawn from the graphical results in Figures IX, X, and XI is that the performance of the S/N gage is virtually unaffected by the mean load. This is somewhat remarkable when one considers that the peak values of strain encountered in the compression tests differed from those in the tension tests by as much as 5000 $\mu\epsilon$. These results mean that the performance curves in Figure II are valid in applications where mean load is not zero, and they also suggest that the influencing factor is peak-to-peak strain rather than plastic strain. Peak-to-peak strain has been proposed by Gross (4) as a fatigue criterion.

It can be further concluded from the experimental results that the S/N gage is limited in actual application to those phases of fatigue which take place prior to crack initiation. Cracking in the surface causes redistribution of strain which impairs the gage reliability. Furthermore, if a crack forms directly under the gage, the gage will probably fail instantly because the backing material is quite brittle. Formation of fatigue cracks is accompanied by the liberation of gas, as Bennett (2) has shown, which factor could possibly cause the adhesive to break underneath

The first division of the report is devoted to a description of the general results of the investigation. The second division is devoted to a description of the experimental methods used. The third division is devoted to a description of the results of the investigation. The fourth division is devoted to a description of the conclusions drawn from the investigation.

It can be further pointed out that the application
should be made to the Board of Directors of the
Company in order to obtain the necessary approval
for the proposed plan. The Board of Directors
should be consulted in order to obtain the
necessary approval for the proposed plan.

the gage and thus affect its performance.

In the preloaded tests, there was some indication that the resistance change of the tension gage was slightly greater than the compression gage, although the results were not absolutely conclusive. The tests at $\pm 1980 \mu\epsilon$ and $\pm 2510 \mu\epsilon$ exhibited this tendency, but in the test at $\pm 1560 \mu\epsilon$, the resistance change was slightly greater in the compression gage. The modulus of elasticity for 2024-T4 aluminum is approximately 2 per cent greater in compression than in tension. In addition to producing slightly greater strain on the tension side of the bending specimen, this property also causes the neutral axis to shift. Strain hardening effects cause shifting of the neutral axis also, which makes it impossible to analyze small differences in surface strain. This problem is an inherent difficulty encountered in reverse bending and rotational bending modes of testing.

The curve shown in Figure V, which is the performance modulus of the S/N gage at constant strain amplitude, actually represents the characteristic shape of each curve shown in Figure II. From the experimental results it can be seen that the characteristic shape of the curves at constant stress amplitude for 2024-T4 aluminum follows the curve in Figure V out to approximately 4×10^4 cycles, after which it falls progressively farther below the curve at

The page was then placed in the envelope.

In the envelope were three other letters dated

the previous month of the letter was also dated

these were the three letters dated, which were placed with

the envelope in the envelope. The letter was dated

1950-1951, which was the letter, but in the year of

1950-1951, the letter was dated and dated, which was

the envelope dated. The letter was dated for 1950-1951

envelope is approximately 1950-1951, which was dated in 1950-1951

year is 1950. It was dated in 1950-1951, which was dated

year is 1950-1951, which was dated in 1950-1951, which

year is 1950-1951, which was dated in 1950-1951, which

year is 1950-1951, which was dated in 1950-1951, which

year is 1950-1951, which was dated in 1950-1951, which

year is 1950-1951, which was dated in 1950-1951, which

year is 1950-1951, which was dated in 1950-1951, which

year is 1950-1951, which was dated in 1950-1951, which

year is 1950-1951, which was dated in 1950-1951, which

year is 1950-1951, which was dated in 1950-1951, which

year is 1950-1951, which was dated in 1950-1951, which

year is 1950-1951, which was dated in 1950-1951, which

year is 1950-1951, which was dated in 1950-1951, which

year is 1950-1951, which was dated in 1950-1951, which

year is 1950-1951, which was dated in 1950-1951, which

year is 1950-1951, which was dated in 1950-1951, which

year is 1950-1951, which was dated in 1950-1951, which

higher values of (n) . While the experimental results were not sufficient in number to accurately determine values of $\left(\frac{\partial \Delta R}{\partial \epsilon}\right)$, an estimate of the characteristic shape is shown in Figure XIII. This curve shows that the performance characteristics at constant strain amplitude can be related to a particular material in a constant stress amplitude application. It will be necessary to have such a response function for a particular material in order to perform spectrum studies in random loading.

Some comments are worthy of mention with regard to the use of the gage. Perforated copper electrical terminal strips which are mounted on fibre glass-epoxy backings were found to perform rather poorly under conditions of alternating strain. The backing is so heavy that it tended to break the adhesive early in the course of a test, and the perforation in the copper terminal produced stress concentrations which, in turn, promoted cracking in the terminal. It was found that the best terminal strips for use with the S/N gage are the solid copper strips which are mounted on a Teflon backing. Furthermore, orienting the terminals so that their long axis is perpendicular to the strain field resulted in greater reliability and longer fatigue life.

The instructions, supplied by the manufacturer for mounting the gage are generally adequate. However, there should be a precautionary note in the instructions regarding

the other hand, the fact that the fundamental structure of

the system is not in any way affected by the change of

the system is not in any way affected by the change of

the system is not in any way affected by the change of

the system is not in any way affected by the change of

the system is not in any way affected by the change of

the system is not in any way affected by the change of

the system is not in any way affected by the change of

the system is not in any way affected by the change of

the system is not in any way affected by the change of

the system is not in any way affected by the change of

the system is not in any way affected by the change of

the system is not in any way affected by the change of

the system is not in any way affected by the change of

the system is not in any way affected by the change of

the system is not in any way affected by the change of

the system is not in any way affected by the change of

the system is not in any way affected by the change of

the system is not in any way affected by the change of

the system is not in any way affected by the change of

the system is not in any way affected by the change of

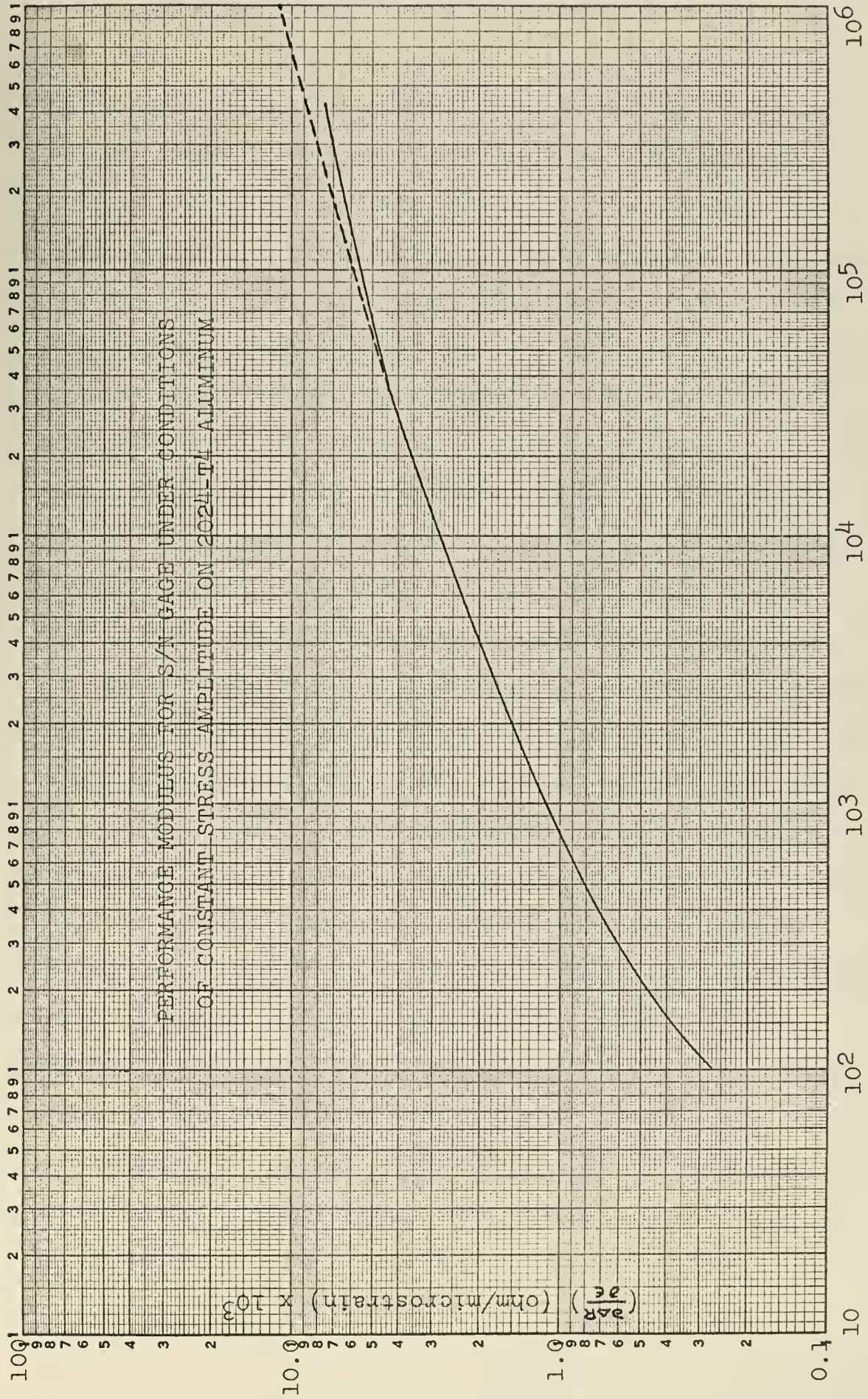
the system is not in any way affected by the change of

the system is not in any way affected by the change of

the system is not in any way affected by the change of

the system is not in any way affected by the change of

the system is not in any way affected by the change of



n (cycles)

FIGURE XIII

attachment of the jumper wires between the gage and the terminal strips. Solder does not wet the S/N gage grid material. There is a small button on each terminal which is about the size of a pin head, and this button provides the only location where the jumper wire can be attached. The instructions should caution the user to be very careful when cleaning these points for tinning since they cannot withstand more than the slightest amount of abrasion. Furthermore, the jumper wires should be attached to the terminal strips before they are connected to the gage because the contact points on the gage are very fragile and easily sheared off. If this happens, the gage is rendered useless.

Because the gage backing material is rigid, it must be roughened before attaching to a specimen or structure. This is accomplished by lapping the bonding surface with pumice or similar abrasive. The technique of lapping the gage is a delicate one, since too little roughening results in the gage not bonding properly and too much ruins the gage. Several gages parted from specimens during the experimental testing, but in all cases the adhesive parted from the specimen rather than from the gage. It is believed that this problem occurred because of the characteristic oxide film which forms on aluminum surfaces and also because the machine marks on the test specimens were purposely made to run in the direction of the strain field. Those specimens which

fractured as a result of fatigue failed well beyond their expected fatigue limits. It appears that additional specimen life was obtained at the expense of reduced gage life in these experimental tests.

There are numerous practical applications in which alternating strains occur at some mean level of strain. In a submarine pressure hull, for example, the alternating loads are purely compressive or tensile in nature. And an aircraft wing in flight buffets about the mean loading imposed by aerodynamic lift. In using the S/N gage to monitor cumulative fatigue under these conditions, several factors must be considered when relating the gage's performance to structural damage. Fatigue strength of the material is reduced by imposing a mean loading condition. Experimental results show that the S/N gage will not be significantly affected by mean loading. And if the structure experiences any plastic deformation, the gage behaves as a strain gage and will indicate a change in electrical resistance. It was previously pointed out that the gage functions whether monitored continuously or periodically, but since gage response is not uniform throughout its life span and until such time as sufficient information on the gage's performance has been acquired, it will be beneficial to monitor the gage as much and as often as the limitations of a particular application permit.

In the work which has so far been done with the S/N

The first of these is the fact that the
 system is not a simple one. It is a
 complex one, and it is not possible to
 describe it in a few words. It is a
 system which is based on the principle of
 the conservation of energy. It is a
 system which is based on the principle of
 the conservation of momentum. It is a
 system which is based on the principle of
 the conservation of angular momentum. It
 is a system which is based on the
 principle of the conservation of the
 total energy of the system. It is a
 system which is based on the principle of
 the conservation of the total momentum of
 the system. It is a system which is
 based on the principle of the conservation
 of the total angular momentum of the
 system. It is a system which is based
 on the principle of the conservation of
 the total energy, total momentum, and
 total angular momentum of the system.

gage, emphasis has been placed on developing it as an engineering tool for monitoring cumulative fatigue damage. The results of this investigation show that the gage may also prove to be a valuable laboratory tool. In part III it was shown that there is a powerful analogy between changes in electrical resistivity of the gage and the fatigue mechanism. Applying this analogy showed that, among other things, the endurance limit of the gage may possibly decrease slightly over the total fatigue life. It was further brought out in the experimental results that the effects of a particular material and testing method can be distinguished by their influence on the gage's performance modulus. The important point to be made here is that the gage can be used for isolating and determining the magnitude of individual factors in studying the complicated problem of fatigue.

VIII. APPENDIX

A. DETAILS OF PREPARING THE BENDING SPECIMENS

All of the specimens used in the reverse bending tests were fabricated from 3/16" x 2" 2024-T4 aluminum bar stock. Ten-inch lengths of stock were marked and cut approximately to form with a metal band saw. Then they were filed to shape and carefully smoothed with fine emery cloth. Great care was taken to insure that all the machine marks ran parallel to the long dimension of the specimen so as to minimize the possibility of transverse cracking.

After each specimen had been shaped and smoothed, it was cleaned with trichloroethylene to remove all oils and soluble material. The surface on which each gage was mounted was prepared with Bean Metal Conditioner using 180 grit silicon carbide paper, after which it was cleaned with ammonia neutralizer and wiped dry.

One strain gage was installed on each specimen using Eastman 910 cement and standard installation procedures. The S/N fatigue gages were mounted with Eastman 910 also, but the procedure was slightly more involved. Prior to mounting, the backing surface of each S/N gage was lapped using fine pumice and clean paper on a glass plate. Each of the electrical terminal strips was lapped in this same manner, also. The gage and terminal strip backs were then cleaned with ammonia neutralizer to remove any traces of

pumice, after which they were joined to the specimen using the same techniques as those employed in mounting the strain gages.

With the gages attached to the specimen, the terminals were then tinned using a low temperature (300°F) soldering iron. Preparing the terminals on the S/N gage require great care since there is only one contact point in the center of each terminal to which solder will adhere. These points are about the size of a pinhead and solder will not bond to the gage at any other location. Two #34 copper wire jumpers were used to connect the gage terminals to the terminal strips. A lead wire connection of three conductor, vinyl insulated flat cable was run along the edge of the specimen to the terminal strips and cemented in place using a two-part epoxy adhesive. This connector, rather than the terminal strips, served to carry all the weight of the monitoring cables.

Several minor modifications were made to the foregoing procedure for purposes of testing various gage and terminal configurations. As a result of the testing it was found that the best terminal strips to use with the S/N gage were the solid copper strips with a Teflon backing. Furthermore, orienting the terminals so that the long axis is perpendicular to the strain field resulted in greater reliability and longer fatigue life of the electrical connections.

B. DESCRIPTION OF APPARATUS

SF-1U FATIGUE MACHINE

All of the cyclic load tests of the S/N Fatigue Life Gage were performed with a Sonntag Model SF-1U fatigue machine. This machine is an extremely versatile piece of apparatus which can be used to provide alternating loads for fatigue testing in tensile, torsional, or reverse bending configurations.

In principle, the machine's operation is quite simple. The top of the SF-1U is a large flat table, or platen as it is called, made of cast steel and having a very large mass. This platen is suspended from the casing of the machine on turn-buckle springs which permit a small amount of motion in the horizontal direction but which constrain it in the vertical. This large table is called the stationary platen.

In the center of the stationary platen is a smaller rectangular platen whose flat surface is at the same level as the top of the stationary platen. This smaller platen is an integral part of a heavy frame which is suspended from the underside of the stationary platen on heavy springs and is free to move only in the vertical direction. Within this frame is a rotating weight having an off-center mass. The eccentricity of this mass can be adjusted by turning a

threaded shaft. A synchronous motor spins the eccentric weight at exactly thirty revolutions per second which, in turn, produces an alternating force proportional to the mass, the eccentricity, and the square of the rotational speed. Since the framework is constrained horizontally, only the vertical component of alternating force is transmitted to the smaller platen, which, for this reason, is called the vibrating platen.

All of the modes of operation, torsional, tensile, and reverse bending, are accomplished by means of separate attachments which fasten to the two platens of the SF-1U machine. Each attachment converts the sinusoidal force transmitted by the vibrating platen into the desired loading of a test specimen which is anchored to the stationary platen.

In order that all of the alternating forces be transmitted only to the test specimen, the proper 'mass-elastic couple' must exist between the vibrating assembly and the stationary components. To produce this relationship, tuning weights are attached to the vibrating platen carriage. When the system is properly tuned, the amplitude of vibration is at its maximum for a particular eccentric weight setting.

The SF-1U has an automatic preload feature which permits superimposing a known static force on the vibrating platen. This force can be maintained automatically in a preset

amount throughout a test, or the automatic feature can be turned off and the load adjusted manually. It is possible to apply the preload as either a tensile or a compressive force.

There are certain safety and convenience features built into the SF-1U machine. Microswitches stop the machine if the amplitude of the vibrating platen exceeds ± 0.35 inches. And there is fine speed control of the synchronous motor so that it can be brought up to speed without excessively exciting undesirable modes of vibration and producing unwanted transient effects.

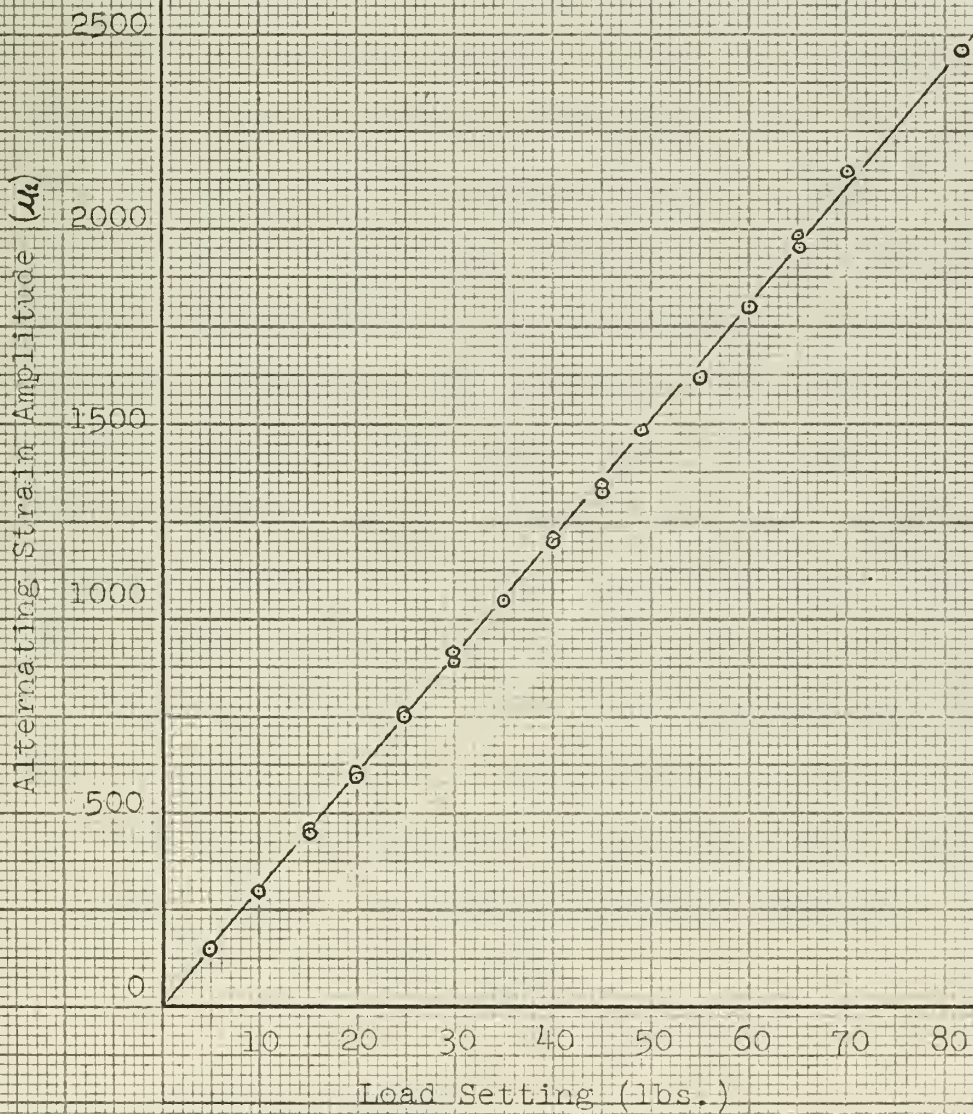
The specified accuracy of the alternating load and the static preload is ± 2 per cent of the amplitude. This is a factory specification which applies to the setting and tuning mechanisms, not to the precision of the machine. Actually, much greater precision can be obtained by the use of instrumented specimens. A calibration of the machine was performed for the particular specimen used in the experimental tests of the S/N gage and is shown in Figure XIV.

REVERSE BENDING FIXTURE

The reverse bending fixture for the SF-1U machine was used to perform all of the cyclic load tests of the S/N fatigue gage. This fixture consists of two rocker arms, each of which are equipped with grips to clamp the ends of

FIGURE XIII

SF-10 FATIGUE MACHINE CALIBRATION CURVE FOR
THE REVERSE BENDING FIXTURE



the specimen. When installed on the SF-1U machine, the ends of the rocker arms pivot about rigid bearings fastened to the stationary platen. The rocker arms also pivot about centrally located, movable bearings which are connected to the vibrating platen. One of the rocker arms is free to move laterally so that no axial force is applied when the specimen is deflected.

With a specimen mounted in the bending fixture, the free length of the bar between the grips can be considered as a beam to which point bending moments are applied at the ends. Each of these alternating moments is equal in magnitude to one-half the product of the alternating force of the vibrating platen and the distance separating the fixed and movable pivots of each rocker arm. This type of loading, usually referred to as "double cantilever loading", produces a bending moment of constant magnitude across the entire span of the specimen between the grips of the rocker arms.

Double cantilever loading has a particular advantage in that no strain gradients are produced in that portion of the specimen where the section is uniform. This feature was a principal reason for choosing reverse bending as a method of testing the R/N fatigue gage.

BAM-1 STRAIN INDICATOR

All of the strain measurements, both static and dynamic, were taken with an Ellis BAM-1 strain indicator. This

one specimen, when installed on the 15-11 machine, the same as the others were given about eight passages between the stationary plates. The second specimen was also given about eight passages, movable handles which are connected to the vibrating plates. One of the plates was fixed to move laterally so that no axial force is applied when the specimen is subjected with a specimen mounted in the device. The distance between the bar between the plates and the specimen is a distance to which point bending moments are applied at the ends. Each of these vibrating elements is equal in magnitude to one-half the product of the vibrating mass of the vibrating plates and the distance separating the plates and movable plates of each section. This type of loading, usually referred to as "double cantilever loading," produces a bending moment of constant magnitude across the entire span of the specimen between the grips of the testing machine. Double cantilever loading has a particular advantage in that no strain gradients are produced in the portion of the specimen where the section is uniform. This feature was a principal reason for choosing double cantilever loading as a method of testing the low tensile strength.

APPENDIX I - DATA

All of the tests were run on a 15-11 machine and the results were taken with an EIMCO strain indicator. This

instrument is a Wheatstone Bridge direct reading strain indicator and also a D.C. amplifier. The latter feature is one which makes it especially adaptable for dynamic measurements since a D.C. component of strain, if present, is not lost in amplifying the strain gage signal. Static strain measurements may be taken by reading a meter on the front of the indicator, but dynamic measurements must be made by means of an oscilloscope presentation. Gain control in both the meter and the oscilloscope permit very fine adjustment and calibration of the BAM-1.

ELH - TYPE N STRAIN INDICATOR

The ELH Type N strain indicator was used for measuring resistance changes of the S/N gage. This device is a Wheatstone Bridge null balance indicator having a range extension feature which permits measuring relatively large values of resistance change. A gage factor setting mechanism facilitates easy calibration of the instrument. This device is extremely accurate for measuring resistance changes in units of strain.

S/N FATIGUE LIFE GAGES

The following information applies to the S/N gages which were used in conducting the experimental work of this

Investigation:

S/N FATIGUE LIFE GAGES

MANUFACTURER: Micro-Measurements, Inc.

TYPE: NA-01

RESISTANCE: $100 \pm 0.2\%$

LOT NUMBERS: A12AP11, A12AP13, and A12AP15

UNIVERSITY OF CALIFORNIA, BERKELEY

DEPARTMENT OF CHEMISTRY

RECEIVED

1954

1954

1954

1954

1954

1954

1954

1954

1954

1954

1954

1954

1954

1954

1954

1954

1954

C. SAMPLE CALCULATIONS

In all of the S/N fatigue gage tests, changes in the gage resistance were measured with a BLH Type N strain indicator. This instrument is a Wheatstone Bridge null-balance device which is designed to measure resistance change in units of strain (microinches per inch). The following expression equates resistance change and indicated strain for a null-balance indicator:

$$\Delta \epsilon_1 = \frac{\Delta R}{R} \times \frac{1}{(\text{Gage Factor})} \quad (8)$$

where $\Delta \epsilon_1$ is the difference between successive readings and R is the total resistance of the gage.

When the BLH indicator is used to measure strain, the gage factor for a particular gage can be set directly into the instrument by means of a dial and the strain read directly. This feature facilitates calibrating the indicator, but because the indicator was not used to measure strain in this application, the gage factor dial was set at 2.00 for all readings in order to simplify the calculations. Under these conditions, equation (8) can be restated in the following form:

$$\Delta R = 2.00 R (\Delta \epsilon_1) \quad (9)$$

2. THEORETICAL BACKGROUND

In all of the following cases, the results are

expressed in terms of the number of states N .

Consider the following cases:

(a) The number of states is N .

(b) The number of states is $N/2$.

(c) The number of states is $N/4$.

(d) The number of states is $N/8$.

(e)

$$E = \frac{1}{2} \log_2 N$$

where E is the entropy of the system.

Consider the following cases:

(a) The number of states is N .

(b) The number of states is $N/2$.

(c) The number of states is $N/4$.

(d) The number of states is $N/8$.

(e) The number of states is $N/16$.

(f) The number of states is $N/32$.

(g) The number of states is $N/64$.

(h) The number of states is $N/128$.

where

(i)

$$E = \frac{1}{2} \log_2 N$$

For very small values of dR (less than 1 per cent of R), the above expression can be used with sufficient accuracy by assuming that R is constant and equal to the initial value of total gage resistance. When larger values of dR are to be computed, however, this assumption results in progressively larger errors due to the non-linear relationship between the initial gage resistance and dR . It will be recalled that the total resistance change of the E/N gage during its useful life is 8 per cent to 10 per cent of the initial gage resistance. In the experimental tests, however, readings were taken at intervals during which the incremental values of resistance change were generally less than 0.5 per cent of the initial gage resistance. In this manner, it was possible to use equation (9) for computing dR by assuming R to be the total gage resistance at the start of a particular increment. This can be expressed by the following recursion formula:

$$dR_n = (R_0 + \sum_{i=1}^{n-1} dR_i) 2.00 (d\epsilon_1) \quad (10)$$

The following relationship was used for computing ΔR , the total resistance change:

$$\Delta R (\%) = 100 \frac{\sum dR}{R_0} \quad (11)$$

It can be seen from this expression that a small error in estimating R_0 results in dR being in error by the same

The first half of the paper is devoted to the study of the asymptotic behavior of the solutions of the system (1) for large values of t . It is shown that the solutions of the system (1) are bounded and oscillate about the origin. The second half of the paper is devoted to the study of the asymptotic behavior of the solutions of the system (1) for small values of t . It is shown that the solutions of the system (1) are bounded and oscillate about the origin. The third half of the paper is devoted to the study of the asymptotic behavior of the solutions of the system (1) for large values of t . It is shown that the solutions of the system (1) are bounded and oscillate about the origin. The fourth half of the paper is devoted to the study of the asymptotic behavior of the solutions of the system (1) for small values of t . It is shown that the solutions of the system (1) are bounded and oscillate about the origin. The fifth half of the paper is devoted to the study of the asymptotic behavior of the solutions of the system (1) for large values of t . It is shown that the solutions of the system (1) are bounded and oscillate about the origin. The sixth half of the paper is devoted to the study of the asymptotic behavior of the solutions of the system (1) for small values of t . It is shown that the solutions of the system (1) are bounded and oscillate about the origin. The seventh half of the paper is devoted to the study of the asymptotic behavior of the solutions of the system (1) for large values of t . It is shown that the solutions of the system (1) are bounded and oscillate about the origin. The eighth half of the paper is devoted to the study of the asymptotic behavior of the solutions of the system (1) for small values of t . It is shown that the solutions of the system (1) are bounded and oscillate about the origin. The ninth half of the paper is devoted to the study of the asymptotic behavior of the solutions of the system (1) for large values of t . It is shown that the solutions of the system (1) are bounded and oscillate about the origin. The tenth half of the paper is devoted to the study of the asymptotic behavior of the solutions of the system (1) for small values of t . It is shown that the solutions of the system (1) are bounded and oscillate about the origin.

$$(11) \quad \frac{d^2 x}{dt^2} + \frac{d^2 y}{dt^2} + \frac{d^2 z}{dt^2} = 0$$

The system (11) is a linear system of three second-order ordinary differential equations. The solutions of the system (11) are bounded and oscillate about the origin.

$$(12) \quad \frac{d^2 x}{dt^2} + \frac{d^2 y}{dt^2} + \frac{d^2 z}{dt^2} = 0$$

The system (12) is a linear system of three second-order ordinary differential equations. The solutions of the system (12) are bounded and oscillate about the origin.

amount and, as such, has a cancelling effect. And because R_0 has a value of 100 ohms, ΔR can be expressed in units of ohms or percentage of initial gage resistance since the numerical values in either case are identical.

D. ORIGINAL DATA

TABLE II

$$\epsilon = \pm 1500 \mu\epsilon$$

$$\epsilon_M = 0$$

ALTERNATING LOAD = 49 lbs.

<u>n (cycles)</u>	<u>$\epsilon_i (\mu\epsilon)$</u>	<u>σ_R (ohms)</u>	<u>ΔR (ohms)</u>
1	35	.007	0.007
10	76	.015	0.022
7,200	1981	.396	0.418
9,200	186	.037	0.455
11,000	249	.038	0.505
14,600	435	.087	0.592
18,200	425	.085	0.677
21,800	395	.079	0.756
27,200	381	.077	0.833
36,200	509	.102	0.935
45,200	428	.086	1.021
65,000	1020	.206	1.227
85,000	672	.136	1.363
112,000	535	.108	1.471
137,000	475	.096	1.567
166,000	490	.099	1.666
189,000	309	.063	1.729
214,600	295	.060	1.789
248,600	377	.077	1.866
272,000	371	.076	1.942
358,000	590	.120	2.062
434,000	221	.045	2.107
488,200	437	.089	2.196
542,000	392	.082	2.276
596,000	320	.060	2.342
654,000	360	.074	2.416
709,000	350	.072	2.488
763,000	290	.060	2.548
818,000	250	.051	2.599
872,000	225	.046	2.645

(Test Terminated Due to Cracking of Terminal Strips)

3. $\frac{1}{2} \times \frac{1}{2} = \frac{1}{4}$

333

TABLE III

$$\epsilon = +1500 \mu\epsilon$$

$$\epsilon_m = -1500 \mu\epsilon$$

ALTERNATING LOAD = 92 lbs.

<u>n (cycles)</u>	<u>$\epsilon_i (\mu\epsilon)$</u>	<u>$\sigma_R (\text{ohms})$</u>	<u>$\Delta R (\text{ohms})$</u>
3,600	886	0.177	0.177
10,800	2040	0.408	0.585
21,600	1365	0.278	0.863
36,000	1470	0.290	1.150
66,600	1345	0.270	1.425
120,600	1580	0.320	1.749
147,600	555	0.113	1.862
174,600	560	0.114	1.876
228,600	750	0.153	2.129
282,600	550	0.114	2.243
336,600	770	0.158	2.401
372,600	160	0.037	2.433

(Test was Terminated Due to Electrical Terminal Failure on the S/N Comp.)

TABLE IV

$$\epsilon = \pm 1560 \mu\epsilon$$

$$\epsilon_M = + 1500 \mu\epsilon$$

ALTERNATING LOAD = 52 LB.

<u>n (cycles)</u>	<u>$\epsilon_i (\mu\epsilon)$</u>	<u>σ_R (ohms)</u>	<u>ΔR (ohms)</u>
3,600	815	0.163	0.163
10,800	2100	0.420	0.583
21,600	1380	0.277	0.860
39,600	1370	0.276	1.136
66,600	1250	0.253	1.389
120,600	1470	0.298	1.687
147,600	575	0.117	1.804
174,600	485	0.099	1.903
228,600	705	0.144	2.047
282,600	535	0.110	2.157
336,600	445	0.091	2.248
372,600	300	0.062	2.310
400,000	320	0.065	2.372
454,000	500	0.102	2.477
508,000	430	0.087	2.564
562,000	400	0.082	2.646
616,000	570	0.177	2.753
668,000	350	0.072	2.835
722,000	360	0.074	2.909

(Test Terminated Due to Cracking of Terminal Strip)

3

CM

Page 3 of 9

TABLE V

$$\epsilon = \pm 2030 \mu\epsilon$$

$$\epsilon_m = 0$$

ALTERNATING LOAD = 65 lbs.

n (cycles)	ϵ_i ($\mu\epsilon$)	ΔR (ohms)	ΔR (in)
1	110	0.022	0.022
1,800	2610	0.523	0.545
3,600	1580	0.320	0.865
5,400	1330	0.268	1.133
7,200	1120	0.227	1.360
9,000	960	0.194	1.554
12,600	1455	0.295	1.849
16,200	1175	0.239	2.088
19,800	948	0.193	2.281
23,400	802	0.164	2.445
28,900	1035	0.212	2.657
34,300	840	0.173	2.830
39,700	755	0.155	2.985
45,100	630	0.130	3.115
54,100	890	0.183	3.298
63,100	785	0.162	3.460
73,900	800	0.166	3.626
92,200	1175	0.244	3.870
110,200	1000	0.208	4.078
139,000	1460	0.304	4.382
169,600	1585	0.331	4.713
207,400	2175	0.455	5.168
245,200	2525	0.531	5.699
254,200	785	0.165	5.864
277,600	3075	0.650	6.514
286,600	1475	0.314	6.828
299,200	1930	0.413	7.241
308,200	1595	0.342	7.583
320,800	2770	0.596	8.179
329,800	2185	0.474	8.653
331,600	790	0.172	8.825
333,400	610	0.133	8.958
344,200	2950	0.643	9.601
353,200	2255	0.494	10.095

(Test Terminated Due to Formation of a Small Blister Under the S/N Gage)

44-38861-3

33

TABLE VI

$$E = \pm 1980 \mu\epsilon$$

$$E_M = -2000 \mu\epsilon$$

ALTERNATING LOAD = 65 lbs.

<u>n (cycles)</u>	<u>d E_i ($\mu\epsilon$)</u>	<u>$\bar{\sigma}R$ (ohms)</u>	<u>ΔR (ohms)</u>
1,800	1925	0.385	0.385
3,600	1195	0.240	0.625
5,400	835	0.168	0.793
7,200	685	0.138	0.931
10,800	1085	0.219	1.150
16,200	1390	0.281	1.431
19,900	1065	0.216	1.647
23,500	765	0.155	1.802
27,100	695	0.142	1.944
36,100	895	0.182	2.126
45,100	785	0.161	2.287
54,100	725	0.148	2.435
72,100	1055	0.216	2.651
90,100	880	0.181	2.832
108,100	780	0.160	2.992
135,000	895	0.184	3.176
162,000	715	0.148	3.324
216,000	1215	0.251	3.575
270,000	1120	0.232	3.807
324,000	970	0.201	4.008
381,600	1205	0.252	4.230
450,000	1625	0.339	4.569
506,000	4435	0.924	5.503

(Specimen Fractured)

TABLE VII

$$\epsilon = \pm 1980 \mu\epsilon$$

$$\epsilon_m = +2000 \mu\epsilon$$

ALTERNATING LOAD = 65 lbs.

<u>n (cycles)</u>	<u>$\epsilon_i (\mu\epsilon)$</u>	<u>$\Delta R (\text{ohms})$</u>	<u>$\Delta R (\text{ohms})$</u>
1,800	2183	0.436	0.436
3,600	1357	0.272	0.708
5,400	1095	0.220	0.928
7,200	760	0.154	1.082
10,800	1320	0.267	1.349
16,200	1485	0.301	1.650
19,900	1105	0.225	1.875
23,500	805	0.164	2.039
27,100	695	0.142	2.181
36,100	920	0.188	2.369
45,100	780	0.160	2.529
54,300	735	0.151	2.680
72,100	1225	0.251	2.931
90,100	950	0.195	3.126
108,100	835	0.170	3.296
135,000	965	0.199	3.495
162,000	790	0.164	3.659
216,000	1445	0.300	3.959
270,000	1440	0.299	4.258
324,000	1455	0.304	4.562

(Specimen Fractured at 506,000 Cycles)

Э

310 10078 - M3

TABLE VIII

$$\epsilon = \pm 2490 \mu\epsilon$$

$$\epsilon_m = 0$$

ALTERNATING LOAD = 82 lbs.

<u>n (cycles)</u>	<u>$\Delta \epsilon_i (\mu\epsilon)$</u>	<u>$\Delta R (\text{ohms})$</u>	<u>$\Delta R (\text{ohms})$</u>
900	3370	0.675	0.675
1,800	1990	0.400	1.075
2,700	2045	0.413	1.488
3,600	1400	0.284	1.772
4,500	1185	0.241	2.013
5,300	1690	0.345	2.358
6,100	1390	0.285	2.643
9,900	1160	0.238	2.881
11,700	940	0.193	3.074
15,300	1540	0.317	3.391
18,900	1230	0.254	3.645
22,500	1050	0.218	3.863
28,000	1260	0.262	4.125
33,000	1070	0.223	4.348
39,000	920	0.192	4.540
44,000	775	0.162	4.702
53,000	1210	0.253	4.955
60,000	850	0.178	5.133
69,000	940	0.198	5.331
79,000	1145	0.241	5.572
88,000	970	0.205	5.777
97,000	1115	0.235	6.012
106,000	1040	0.221	6.233
115,000	980	0.208	6.441
125,000	1165	0.248	6.689
144,000	1815	0.387	7.076
162,000	1855	0.397	7.473
182,000	2290	0.492	7.965
200,000	2365	0.511	8.476
209,000	1560	0.338	8.814
218,000	1490	0.324	9.138
227,000	2150	0.470	9.608
336,000	1625	0.356	9.964

(Test Terminated When Corner of the Gage was Observed to Have Parted From the Specimen)

TABLE 1

31-10-1952 = 0

31-10-1952 = 100

31-10-1952 = 100

31-10-1952

31-10-1952

31-10-1952

31-10-1952

31-10-1952

31-10-1952

31-10-1952

31-10-1952

(The following are the names of the persons who have been in the country since 1-1-1952)

TABLE IX

$$\epsilon = \pm 2510 \mu\epsilon$$

$$\epsilon_M = -2500 \mu\epsilon$$

ALTERNATING LOAD = 82 lbs.

<u>N (cycles)</u>	<u>$\Delta \epsilon_i (\mu\epsilon)$</u>	<u>SR (ohms)</u>	<u>ΔE (ohms)</u>
900	3025	0.605	0.605
1,800	2100	0.423	1.028
2,700	1950	0.334	1.402
3,600	1370	0.270	1.701
4,500	1330	0.271	1.772
5,400	1070	0.218	2.150
7,200	1705	0.348	2.536
9,000	1555	0.319	2.857
10,800	1100	0.226	3.083
12,900	1090	0.225	3.308
14,700	800	0.165	3.473
16,500	710	0.147	3.620
20,100	1192	0.248	3.868
23,700	975	0.202	4.070
27,300	830	0.173	4.243
31,700	1025	0.214	4.457
38,100	875	0.183	4.640
43,500	800	0.167	4.807
52,500	1125	0.235	5.042
61,500	1045	0.218	5.060
70,800	1060	0.223	5.483
80,000	1080	0.226	5.711
89,000	1030	0.218	5.929
99,000	1140	0.241	6.170
117,000	2955	0.626	6.796
133,200	3080	0.656	7.452
145,800	3215	0.690	8.142
155,000	2890	0.624	8.766
168,000	4650	1.011	9.777
188,000	8340	1.830	11.607

(Specimen Fractured at 220,000 Cycles)

3M 1000 M3

TABLE X

$$\epsilon = \pm 2510 \mu\epsilon$$

$$\epsilon_M = +2500 \mu\epsilon$$

ALTERNATING LOAD = 82 lbs.

<u>n (cycles)</u>	<u>$\epsilon_i (\mu\epsilon)$</u>	<u>$R (\text{ohms})$</u>	<u>$\Delta R (\text{ohms})$</u>
900	3670	0.734	0.734
1,800	2480	0.500	1.234
2,700	1840	0.372	1.506
3,600	1500	0.305	1.911
4,500	1260	0.257	2.163
5,300	2320	0.473	2.691
6,100	2040	0.418	3.059
6,900	1300	0.268	3.327
11,700	810	0.168	3.495
13,500	1740	0.360	3.855
15,300	760	0.158	4.013
17,100	680	0.142	4.155
18,900	590	0.123	4.278
20,700	730	0.152	4.430
22,500	470	0.092	4.522

(Test Terminated When S/R Gage Adhesive Parted From the Specimen)

322 12/11/1919

2nd 1000 - M3

B. REFERENCES

1. American Society for Testing and Materials. "A Guide for Fatigue Testing and the Statistical Analysis of Fatigue Data," (STP No. 71-A) A.S.T.M., Philadelphia, 1963.
2. Bennett, J. A. "The Effect of a Fatigue Crack on the Fatigue Strength of an Aluminum Alloy," Naval Engineers Journal, Vol. 72, No. 1 (February, 1960), pp. 41-44.
3. Chironis, N. P. "Changes in Strain Gages," Product Engineering, December 6, 1963, p. 83.
4. Gross, M. R. "Low-Cycle Fatigue of Materials for Submarine Construction," Naval Engineers Journal, Vol. 75, No. 4, (October, 1963), pp. 763-777.
5. Hastings, D. M. "The S/N Fatigue Life Curve: A Direct Means of Measuring Cumulative Fatigue Damage," A technical paper presented at the Second International Congress on Experimental Mechanics, September 28, 1965.
6. Sweeney, H. (ed.). Handbook of Experimental Stress Analysis. New York: Wiley & Sons, Inc., 1955.
7. Hume-Rothery, W. Electrons, Atoms, Metals, and Alloys. New York: Dover Publications, Inc., 1963.
8. Kennedy, A. J. Processes of Fatigue and Creep in Metals. London: Oliver & Boyd, Ltd., 1962.
9. Lipson, Charles, and Juvinall, R. C. Handbook of Stress and Strength. New York: The Macmillan Company, 1963.
10. Manson, J. S. "Fatigue: A Complex Subject--Some Simple Approximations," Experimental Mechanics, Vol. 5, No. 7, (July, 1965), pp. 193-226.
11. Morrow, J. Dain. "Cyclic Plastic Strain Energy and Fatigue of Metals," Internal Friction, Damping, and Cyclic Plasticity, (STP No. 378) A.S.T.M., 1965, pp. 45-67.
12. Murray, W. M. (ed.). Fatigue and Fracture of Metals. Cambridge, Mass.: Technology Press, M.I.T., and New York: John Wiley & Sons, Inc., 1952.

CONTENTS

1. Introduction
2. The History of the
3. The
4. The
5. The
6. The
7. The
8. The
9. The
10. The
11. The
12. The
13. The
14. The
15. The
16. The
17. The
18. The
19. The
20. The

13. Sines, George, and Waisanen, J. L. (eds.). Metal Fatigue.
New York: McGraw-Hill Book Co., Inc., 1959.
14. Tavernelli, J. P., and Coffin, L. W., Jr. "A Compilation
and Interpretation of Cyclic Strain Fatigue Tests on
Metals," Transactions of American Society of Metals,
Vol. LI, (1959), pp. 436-453.

9 AUG 66	DISPLAY
13 MAY 69	17557
8 SEP 69	S10069
21 SEP 69	17557
13 NOV 69	17557
25 NOV 69	17557
17 DEC 69	17504

Thesis
T797 Triebes

An investigation of
the S/N fatigue gage.

9 AUG 66	DISPLAY
13 MAY 69	17557
8 SEP 69	S10069
21 SEP 69	17557
13 NOV 69	17557
25 NOV 69	17504

Thesis
T797 Triebes

An investigation of
the S/N fatigue gage.

thesT797

An investigation of the S/N fatigue gage



3 2768 002 03643 6

DUDLEY KNOX LIBRARY